



Published in final edited form as:

New Phytol. 2023 June ; 238(6): 2460–2475. doi:10.1111/nph.18918.

A Role for Ethylene Signaling and Biosynthesis in Regulating and Accelerating CO₂- and ABA-mediated Stomatal Movements in Arabidopsis

Tamar Azoulay-Shemer^{1,2,*}, Sebastian Schulze^{1,*}, Dikla Nissan-Roda², Krystal Bosmans¹, Or Shapira², Philipp Weckwerth¹, Olena Zamora³, Dmitry Yarmolinsky³, Taly Trainin², Hannes Kollist³, Alisa Huffaker¹, Wouter-Jan Rappel⁴, Julian I. Schroeder¹

¹Division of Biological Sciences, Cell and Developmental Biology Section, University of California San Diego, La Jolla, CA 92093-0116, USA.

²Fruit Tree Sciences, Agricultural Research Organization (ARO), The Volcani Center, Newe Ya'ar Research Center, Ramat Yishay, 30095, Israel.

³Plant Signal Research Group, Institute of Technology, University of Tartu, Nooruse 1, Tartu, 50411, Estonia

⁴Department of Physics, University of California San Diego, La Jolla, CA 92093-0116, USA.

Summary

- Little is known about long-distance mesophyll-driven signals that regulate stomatal conductance. Soluble and/or vapor-phase molecules have been proposed. In this study, the involvement of the gaseous signal ethylene in the modulation of stomatal conductance in *Arabidopsis thaliana* by CO₂/ABA was examined.
- We present a diffusion model which indicates that gaseous signaling-molecule/s with a shorter/direct diffusion pathway to guard cells are more probable for rapid

Authors for correspondence: 1) Julian I. Schroeder, Tel: +1 858 534 7759, jischroeder@ucsd.edu, 2) Tamar Azoulay-Shemer, Tel: +972 (0) 4-9539575, shemer.tamar@volcani.agri.gov.il.

*These authors contributed equally.

Author Contributions

This research was planned and outlined by JIS, TA-S, W-JR and SS; JIS, TA-S and SS, DY and HK planned and designed the research; WJR constructed and solved the mesophyll-epidermis diffusion model; TA-S, AH and SS conducted ethylene production analyses; TA-S, SS, KB, DNR, OS, OZ, PW, DY and TT conducted experiments and analyzed the data; JIS, TA-S, SS and WJR led the writing with contributions by the authors. TA-S and SS contributed equally to this work.

Competing interests

None declared.

Supporting Information

The following Supporting Information is available for this article:

Fig. S1 Ethylene production is lower in the high-order *acs* mutants in response to elevated and low [CO₂].

Fig. S2 CO₂-induced stomatal movements are severely affected in *acs* octuple mutant plant leaves but not in the *acs* sextuple and *acs* septuple mutants.

Fig. S3 Leaves of the ethylene overproducer, *eto1-1*, show intact CO₂-induced stomatal conductance responses.

Fig. S4 Leaves of the ethylene insensitive signaling mutant, *ein2-1*, show intact CO₂-induced stomatal conductance responses.

Fig. S5 Leaves of the dominant ethylene insensitive receptor mutants, *etr1-1* and *etr2-1*, show intact CO₂-induced stomatal conductance responses.

Fig. S6 Leaves of intact *etr1-6;etr2-3* double mutant and *etr1-6* single mutant plants show accelerated stomatal opening and closing and an enhanced magnitude of stomatal conductance responses to [CO₂] shifts.

Dataset S1: Raw data.

mesophyll-dependent stomatal conductance changes. We, therefore, analyzed different Arabidopsis ethylene signaling and biosynthesis mutants for their ethylene production and kinetics of stomatal responses to ABA/[CO₂]-shifts.

- According to our research, higher [CO₂] causes Arabidopsis rosettes to produce more ethylene. An ACC-synthase octuple mutant with reduced ethylene biosynthesis exhibits dysfunctional CO₂-induced stomatal movements. Ethylene-insensitive receptor (gain-of-function), *etr1-1* and *etr2-1*, and signaling, *ein2-5* and *ein2-1*, mutants showed intact stomatal responses to [CO₂]-shifts. Whereas loss-of-function ethylene receptor mutants, including *etr2-3;ein4-4;ers2-3*, *etr1-6;etr2-3* and *etr1-6*, showed markedly accelerated stomatal responses to [CO₂]-shifts. Further investigation revealed a significantly impaired stomatal closure to ABA in the ACC-synthase octuple mutant and accelerated stomatal responses in the *etr1-6;etr2-3*, and *etr1-6*, but not in the *etr2-3;ein4-4;ers2-3* mutants.
- These findings suggest essential functions of ethylene biosynthesis and signaling components in tuning/accelerating stomatal conductance responses to CO₂ and ABA.

Keywords

abscisic acid; CO₂; diffusion modeling; ethylene; mesophyll; stomatal conductance

Introduction

Stomata regulate gas-exchange between the atmosphere and the interior of the leaf by guard cell turgor regulation. Stomatal movements allow the controlled uptake of CO₂ for photosynthesis while limiting water-loss through transpiration. Physiological and environmental stimuli, including CO₂ concentration [CO₂], abscisic acid (ABA), ozone, humidity, light, and pathogens, affect stomatal movements (Kim *et al.*, 2010; Kollist *et al.*, 2014; Murata *et al.*, 2015; Assmann & Jegla, 2016).

Leaf mesophyll is the main photosynthetic and carbon-fixing tissue in C3 plants. The intercellular CO₂ concentration (C_i) in leaves is determined by the rates of mesophyll photosynthesis (Lawson *et al.*, 2008; Mott, 2009), mesophyll respiration (Hanstein & Felle, 2002; Busch *et al.*, 2020), stomatal conductance, and the atmospheric CO₂ concentration (Farquhar *et al.*, 1980). Elevated C_i concentrations induce stomatal closure, whereas reduced C_i levels cause stomatal opening (Mott, 1988; Hetherington & Woodward, 2003; Zhang *et al.*, 2018). Several studies have supported the existence of mesophyll-driven signals that travels from the mesophyll to the epidermal layer, thus contributing to the regulation of stomatal conductance (Wong *et al.*, 1979; Lee & Bowling, 1995; Mott, 2009; Fujita *et al.*, 2013). Mesophyll-derived signals have been proposed to include an aqueous signal, which is transferred through the apoplast (Else *et al.*, 1996; Fujita *et al.*, 2013), as well as a vapor-phase signal (Sibbernsen & Mott, 2010; Mott *et al.*, 2014). Various low-molecular-weight compounds function as inducers of stomatal movements and as mediators of signaling in guard cells, including sugars (Flütsch *et al.*, 2020) and plant hormones (Daszkowska-Golec & Szarejko, 2013).

H₂O₂ is a low-molecular-weight molecule which has been suggested to play a role as a secondary messenger during bicarbonate-induced stomatal closure. Chater *et al.* (2015) and Kolla *et al.* (2007) showed that NADPH oxidases AtRBOHD and AtRBOHF can affect high CO₂-induced stomatal closing thus implicating reactive oxygen species as diffusible molecules in CO₂ signaling. However, recent studies using two approaches have shown wild-type-like CO₂-induced stomatal closing kinetics in intact leaves of *atrbohdf* double mutants (Hsu *et al.*, 2018). Together these studies indicate a conditional role of NADPH oxidases in the stomatal CO₂ response.

Recent research has suggested that the phytoactive volatile methyl-jasmonate (MeJA) could also be involved in high [CO₂]-mediated stomatal closure (Geng *et al.*, 2016). Yet, recent independent studies showed largely wild-type-like stomatal movement responses in intact leaves and in intact rosettes of plants of JA synthesis-, JA-receptor and JA-signaling mutant plants in response to environmental factors, including [CO₂] and ozone (Zamora *et al.*, 2021), indicating that an additional gaseous signal may be required for CO₂ signaling.

Based on stomatal aperture imaging, the gaseous hormone ethylene was reported to be involved in the regulation of stomatal movements in response to ozone, drought and ABA (Dodd, 2003; Pospíšilová, 2003; Tanaka *et al.*, 2005; Tanaka *et al.*, 2006; Wilkinson & Davies, 2009). Yet, the effect of ethylene on stomatal movements is ambiguous. In some investigations, ethylene has been shown to induce stomatal opening, while in others it induced stomatal closure (Levitt *et al.*, 1987; Desikan *et al.*, 2006; Iqbal *et al.*, 2011). Moreover, ethylene have been proposed to inhibit the effect of ABA-induced stomatal closure (Tanaka *et al.*, 2005). A role for ethylene has not been demonstrated in stomatal conductance responses to CO₂ concentration changes. To address this question, we investigated the possible roles of ethylene in CO₂-regulated stomatal movements in the present study.

Ethylene originates from the amino acid methionine, which is converted to S-adenosyl-methionine (AdoMet) by AdoMet synthetase. The rate-limiting ACC synthase enzymes (ACS) convert AdoMet to 1-aminocyclopropane-1-carboxylic acid (ACC) (Wang *et al.*, 2002; Pattyn *et al.*, 2021). ACC is then oxidized by ACC oxidases (ACO) into ethylene, CO₂, and cyanide. The Arabidopsis genome encodes twelve annotated ACS isoforms, nine of them shown to be enzymatically active (Yamagami *et al.*, 2003).

CO₂ regulates ethylene biosynthesis via a complex regulatory system. CO₂ may act as both an inducer and a suppressor of ethylene production, depending on the tissue and the prevailing environmental conditions (Mathooko, 1996). In some cases, it has been suggested that high concentrations of CO₂ inhibit ethylene biosynthesis (Chaves & Tomas, 1984; Oetiker & Yang, 1995); whereas in others induces production (Philosoph-Hadas *et al.*, 1986; Mathooko *et al.*, 1999). CO₂-mediate ethylene production involves various mechanisms, including the transcriptional, translational, and post-translational regulation of ACS (Gorny & Kader, 1996; Mathooko *et al.*, 2001) and ACO (Fernandez-Maculet *et al.*, 1993; Zhou *et al.*, 2002).

Ethylene is perceived by binding to five receptors in Arabidopsis: ETHYLENE RESPONSE 1 (ETR1), ETR2, ETHYLENE RESPONSE SENSOR 1 (ERS1), ERS2, and ETHYLENE INSENSITIVE 4 (EIN4) (Gallie, 2015). These receptors function as negative regulators suppressing ethylene signaling. Thus, dominant gain-of-function ethylene receptor mutants cause ethylene-insensitivity, whereas recessive loss-of-function ethylene receptor mutants cause constitutive ethylene signaling (Hua & Meyerowitz, 1998; Binder *et al.*, 2006; Gao *et al.*, 2008; Kim *et al.*, 2011). Downstream, the ethylene receptors associate with and signal to the Raf-like CONSTITUTIVE TRIPLE RESPONSE1 serine/threonine kinase (CTR1) (Kieber *et al.*, 1993; Gao *et al.*, 2003). In the absence of ethylene, CTR1 phosphorylates and inactivates EIN2 (Kieber *et al.*, 1993; Clark *et al.*, 1998). EIN2 encodes for the N-ramp like protein ethylene insensitive 2 protein, which mediates ethylene signaling by the activation of downstream transcriptional ethylene responses (Alonso *et al.*, 1999; Ju *et al.*, 2012; Qiao *et al.*, 2012). Ethylene inhibits its receptors, leading to lowered activity of CTR1, which results in active EIN2 and the transcriptional activation of ethylene-responsive genes (such as ETHYLENE RESPONSE FACTORS, the ERF family) via EIN3/EIN3-like transcription factors (Ju *et al.*, 2012; Qiao *et al.*, 2012; Wen *et al.*, 2012).

In the present study, diffusion modeling analyses support the hypothesis that diffusible gaseous signals from the mesophyll could be involved in regulating stomatal conductance. Hence, we pursued a detailed, comprehensive investigation to explore the role of ethylene in CO₂-induced stomatal movements. Our data show that elevated [CO₂] leads to increased ethylene production in Arabidopsis rosette leaves. Leaves of *acs* (ACC synthesis) octuple mutant plants (Tsuchisaka *et al.*, 2009) were defective in both high CO₂-mediated stomatal closing and low CO₂-induced stomatal opening. The ethylene-insensitive receptor mutants, *etr1-1* and *etr2-1*, and the ethylene-insensitive signaling mutants, *ein2-5* and *ein2-1*, showed intact CO₂-induced stomatal conductance responses. On the other hand, ethylene receptor hypersensitive mutants, including *etr2-3;ein4-4;ers2-3*, *etr1-6;etr2-3* and *etr1-6*, showed enhanced and accelerated stomatal conductance changes in response to [CO₂]-shifts. Positive correlation was found between the impaired or accelerated/enhanced stomatal conductance responses to [CO₂]-shifts and ABA in the *acs* octuple mutant and the loss-of-function receptor mutants *etr1-6;etr2-3*, respectively. The role of ethylene in stomatal conductance responses is discussed.

Materials and Methods

Mesophyll-epidermis diffusion model construction

The diffusion of a molecule C in the domain $0 \leq x \leq L$, where 0 corresponds to the mesophyll site of production, is described by the one-dimensional diffusion equation $dC/dt = D d^2C/dx^2$. Here, L is the distance between mesophyll and epidermis, and D is the diffusion constant. This equation needs to be supplemented with boundary conditions at $x = 0$ (mesophyll) and $x = L$ (epidermis): $DdC/dx = -F$ and $DdC/dx = -\alpha C(L)$, respectively (Chen *et al.*, 2009). In these equations, F represents the constant production of C at the source (mesophyll), and α is the absorption rate at the epidermis. Finally, as the initial condition, we take $C(x,0)=0$. This problem can be solved exactly, with the following solution

$$C(x, t) = C_{eq}(x) - \frac{2FL}{D} \sum_{n=1}^{\infty} \frac{A_n \cos\left(\frac{\beta_n x}{L}\right) e^{-\frac{D\beta_n^2 t}{L^2}}}{\beta_n^2}$$

where $C_{eq}(x) = \frac{F}{\alpha} + \frac{F(L-x)}{D}$ is the steady-state solution, valid for long times. In this formula, β_n are the roots of the equation $\beta \tan(\beta) = \alpha L/D \equiv B$ and the coefficients A_n are given by $A_n = (\beta_n^2 + B^2)/(\beta_n^2 + B^2 + B)$. The solution shows that the dynamics of the molecule C does not depend on F and its value is irrelevant for a comparison of its time dependence as a function of the diffusion constant D . For this reason, we present our computational results in terms of the normalized solution C/C_{eq} .

For large values of D , such that $B \ll 1$, the first root is very small while each subsequent root is increased by approximately π : $\beta_1 \approx \sqrt{B} \ll 1$, $\beta_n = \beta_1 + n\pi$ for $n > 2$. Then, only the first term in the sum of the solution is important and $A_1 \approx 1/2$. In this case, the concentration is approximately uniform within the entire domain, independent of D , and given by

$$C(t) \approx \frac{F}{\alpha} \left(1 - e^{-\frac{\alpha}{L} t}\right)$$

Plant materials and mutant lines

Experiments in this study used the *Arabidopsis thaliana* (L.) Heynh. accession Columbia (Col-0). The following mutants were investigated and ordered from ABRC unless stated otherwise: three different higher-order ACC synthase (ACS) mutants, *acs* sextuple (cs16649: *acs2-1; acs4-1; acs5-2; acs6-1; acs7-1; acs9-1*), *acs* septuple (cs16650: *acs1-1; acs2-1; acs4-1; acs5-2; acs6-1; acs7-1; acs9-1*) and *acs* octuple (cs16651: *acs* sextuple mutant silenced in *acs8* and *acs11* (amiR)) mutants (Tsuchisaka *et al.*, 2009). Gain-of-function mutants *etr1-1* (CS237, AT1G66340), *etr2-1* (CS67924, AT3G23150) (Hua & Meyerowitz, 1998). Loss-of-function mutants, the single mutant *etr1-6* (CS72570, AT1G66340) the double mutant *etr1-6; etr2-3* (Hua & Meyerowitz, 1998) and the triple mutant *etr1-6; ein4-4; ers2-3* (CS71770) were kindly provided by B. Binder (University of Tennessee, USA). Mutant lines in *ein2-1* (AT5G03280), and *ein2-5* (Alonso *et al.*, 1999), were kindly provided by J. Alonso (NC State University, USA). *ein2-1* (CS3071) and the ethylene overproducing mutant *eto1-1* (CS3072, AT3G51770) (Chae *et al.*, 2003) were also analyzed.

Plant growth conditions

Arabidopsis thaliana seeds were surface sterilized (Au - Lindsey Iii *et al.*, 2017). Seeds were stratified for two days at 4°C and germinated under sterile conditions on 1/2 strength MS medium dissolved in 0.8% (w/v) agar, 0.8% (w/v) sucrose (pH 5.8 with 1 N KOH). 10-day-old seedlings were transferred to soil (Sunshine Professional Blending, UC San Diego, USA) / (Even Ari Green 7611 *Arabidopsis*-Blending, Volcani Center, Israel), including Osmocote fertilizer. All plants were grown in controlled Conviron growth chambers under a 12h photoperiod, $\sim 150 \mu\text{mol m}^{-2} \text{s}^{-1}$ light intensity, 21°C and relative humidity of 50–60%

(UC San Diego, USA) or Percival (Volcani Center, Israel) growth chambers under a uniform temperature of 19°C during the dark period and 21°C during the light period, relative humidity of 60–80% under $\sim 150\text{--}180\mu\text{mol m}^{-2}\text{ s}^{-1}$ photon flux density. The *Arabidopsis* plants for gas exchange experiments in Tartu were grown as described in (Zamora *et al.*, 2021)

Ethylene production quantification

Ethylene production was quantified in four- to five-week-old plants grown under ambient CO₂ conditions. On the day of experiments, intact potted plants were incubated in a CO₂-controlled growth chamber for 90 min under low (150 ppm) or high (900 ppm) [CO₂]. Aerial plant parts were excised, placed in 15ml falcon tubes that was immediately plugged with a rubber cap. 90 min later, ethylene was measured by gas-chromatography (5890A HEWLETT PACKARD GAS Chromatograph, CA) using a short 1-m column (13018-U, 80/100 μm Hayesep Q; Supelco) with flame ionization detection and calculated curve reading using a standard to Schmelz *et al.* (2003).

Time-resolved stomatal conductance measurements

Time-resolved stomatal conductance measurements on five- to six-week-old *Arabidopsis* plants were performed on the 5th/6th fully expanded true leaf using the infrared (IRGA)-based gas-exchange analyzer systems LI-6400, LI-6400XT, and LI-6800 with a leaf fluorometer chamber (LI-COR Biosciences, Lincoln, NE, USA), under constant conditions: photon flux density of $150\text{ mol m}^{-2}\text{ s}^{-1}$ (10% blue), temperature of 21°C, and 60–65% relative humidity. In all experimental setups, wild-type and mutant plants were cultivated side by side under identical growth conditions. Stomatal responses to [CO₂]-shifts were investigated as follows: Stomatal conductance was first stabilized at ambient [CO₂], as indicated in each figure (i.e., 360/400 ppm) for 30 min. Then [CO₂] was adjusted to high (800 ppm) or low (100 ppm) levels, followed by another shift to 100 or 800 ppm. Data presented show the means of $n = 3$ intact leaves from individual plants \pm SEM. Relative stomatal conductance was calculated by normalizing each stomatal conductance to the steady-state stomatal conductance under ambient [CO₂].

Whole-plant stomatal conductance responses were measured in an eight-chamber gas-exchange device (Kollist *et al.*, 2007) developed by PlantInvent Ltd (<https://www.plantinvent.com/>). *Arabidopsis* plants at the age of 3–4 weeks were inserted into the gas-exchange cuvettes, incubated for 1 h for stabilization of stomatal conductance. The standard conditions in the chambers were as follows: ambient [CO₂] (400 ppm), $250\mu\text{mol m}^{-2}\text{ s}^{-1}$ light intensity, $\sim 65\%$ relative air humidity, 24°C.

ABA treatment

ABA-induced stomatal closure was tested using the following two protocols as indicated in the legends of Figures 9 and 10). 1) Experiments conducted at UCSD (CA, USA) and at ARO (Newe Ya'ar, Israel) used a petiole-feeding protocol (Ceciliato *et al.*, 2019). 2) Experiments conducted at the University of Tartu (Estonia) were conducted as described in (Zamora *et al.*, 2021).

Results

Diffusion modeling of small molecules inside leaves

Previous research has shown that an unknown diffusible molecule from the mesophyll amplifies the stomatal CO₂ response (Lee & Bowling, 1992; Lee & Bowling, 1995; Fujita *et al.*, 2013; Mott *et al.*, 2014; Fujita *et al.*, 2019). Therefore, we investigated whether soluble or gaseous signals may have theoretical advantage over soluble molecules in mediating the mesophyll to guard cell component of the stomatal movement response. To this end, we studied a diffusion model that simplifies the detailed geometry of the leaf and describes diffusion between the mesophyll and the epidermis along a line connecting the two surfaces. This reduction in complexity allowed us to derive an exact solution for the resulting one-dimensional diffusion problem. This solution is expressed as an infinite sum and enabled us to compute the concentration C as a function of time and parameters at any location between the mesophyll and guard cells at the leaf epidermis. Furthermore, it enabled us to determine limitations on the size, diffusion constants, and distances to stomata in possible rapid regulation of stomatal movements by signals emanating from the mesophyll.

The steady-state solution of the diffusion problem depends on four parameters, the diffusion coefficient D , the absorption rate of the small molecule in guard cells α , the distance from the mesophyll to the guard cells L , and the production rate of the small molecule at the mesophyll F . The dynamics of the solution depends only on the first three parameters and determine how fast the concentration changes at the guard cells/epidermal surface. The diffusion coefficient in liquids depends on the size of the molecule and decreases for larger molecular weight M . For spherical molecules, this is approximated by the Stokes-Einstein equation with $D \sim M^{-1/3}$ (Chandrasekhar, 1943) and is more complex for proteins (Young *et al.*, 1980), as the signal may conceivably be a peptide. The diffusion coefficient is orders of magnitude larger for gases in air than molecules in water (Haynes, 2016). The diffusion rate in plant cell walls has been shown to be relatively slow, with diffusion coefficients for carboxylic acids to be ~1–2 orders of magnitude smaller than in water (Kramer *et al.*, 2007).

Absorption at the epidermal surface corresponds to the flux of molecules into the epidermis/guard cells. Thus, it describes how many molecules enter the cells per unit time and per area by multiplying the concentration at the epidermal surface with the absorption rate α . This rate α can vary over a wide range and depends on the size, hydrophobicity, transport activities and charge of the molecule (Wheeler & Levreault, 1985).

For example, for the epidermal cell plasma membrane of barley leaves, the absorption rate α was quantified for a variety of solutes and was found to be in the range of 0.1–1000 $\mu\text{m}/\text{min}$ (Daeter & Hartung, 1993). Based on three-dimensional imaging, the total thickness of Arabidopsis leaves (~22 day-old) is ~175 μm , where the thickness of the spongy mesophyll is ~40 μm , palisade mesophyll is ~110 μm , and the abaxial and adaxial epidermis thicknesses are ~12 μm and ~14 μm respectively. Based on these values, the mesophyll-epidermis distance L can be as small as ~40 μm , which would be an appropriate value for gaseous diffusion from spongy mesophyll cells to abaxial epidermis guard cells. However, L can be significantly larger for soluble molecules that diffuse via a complex cell wall pathway and can be >100 μm or more (Wuyts *et al.*, 2010). Note that this distance

may be even larger, particularly for the diffusion of soluble molecules through the cell wall, as the cell-wall diffusion path is determined by the complex structure and arrangement of the spongy and palisade mesophyll cells within the tissue. Furthermore, signals may be emanating from the upper palisades to the lower epidermis.

We first investigated the dynamics of the epidermal (guard cell) surface concentration $C(L,t)$ for a fixed value $D=450\mu\text{m}^2/\text{s}$, typical for small molecules in solution, including abscisic acid (264 g/mol) or malate (134g/mol), with molecular weights up to 500 g/mol (Haynes, 2016). In Fig. 1a, we plot the concentration of the small molecule $C(L,t)$, normalized by its steady-state value C_{eq} , as a function of time after a change in $[\text{CO}_2]$ for different mesophyll to epidermis distances L . Here, the absorption rate at the epidermis was set to $a=5\mu\text{m}/\text{min}$. Note that since we rescaled by C_{eq} the solution is independent of the value of F . As expected, the concentration C reaches a steady-state at the guard cell surface much faster for a smaller than for a larger mesophyll to epidermis distance L (Fig. 1a).

The analytical solution for the concentration of the molecule at the epidermis $C(L,t)$ (guard cells) also allowed us to investigate the dependence of the concentration on the diffusion constant. The analytical solution revealed that if the diffusion constant is much larger than the product of the absorption rate (a) and the diffusion distance (L), i.e., $D \gg aL$, the concentration within the space between the mesophyll and epidermis is almost spatially uniform. In other words, diffusion is so fast that any spatial non-uniformities will be quickly reduced. In this case, a solution for the concentration as a function of time $C(t)$ is independent of the diffusion constant D and depends primarily on the absorption rate and distance between the epidermis and mesophyll. This is illustrated in Fig. 1b, where we have plotted the dynamics of C/C_{eq} for a range of values for D and for fixed $L=100\mu\text{m}$. For the largest value of D ($D=450\mu\text{m}^2/\text{s}$), the dynamics of C is indistinguishable from the approximate analytical solution derived in Methods. Thus, even larger values of D , including values consistent with gaseous molecules more rapidly diffusing in air, such as CO_2 ($D=1.09 \times 10^7\mu\text{m}^2/\text{s}$) (Winn, 1950) or ethylene ($D=1.37 \times 10^7\mu\text{m}^2/\text{s}$) (Pritchard & Currie, 1982), do not result in a predicted faster increase in C . The same conclusion can be drawn if one would consider gaseous diffusion in water vapor with high humidity as found inside leaves, as humidity would not sufficiently affect gaseous diffusion constants (Astrath *et al.*, 2009). In Fig. 1b, we have also plotted the dynamics of C for $D=1\mu\text{m}^2/\text{s}$, $D=5\mu\text{m}^2/\text{s}$, and $D=50\mu\text{m}^2/\text{s}$ (black, red, and blue curves). These values were motivated by experimental studies that showed that diffusion of a soluble molecule through the cell wall is 1 to 2 orders of magnitude smaller than in water (Kramer *et al.*, 2007). For these smaller values ($D=1\mu\text{m}^2/\text{s}$, $D=5\mu\text{m}^2/\text{s}$), the increase in the concentration of the small molecule C at the epidermal surface is clearly much slower than for the larger values corresponding to diffusion in water or air (Fig. 1b). Taken together, these results suggest that for values of D corresponding to small molecules in solute or gaseous molecules, the diffusive path length L is the most critical parameter for the time-dependence of the epidermal surface concentration (Fig. 1a). Furthermore, the difference in path lengths for a gaseous molecule in the intercellular spaces of leaves and for a soluble molecule diffusing via complex cell walls, together with the much smaller diffusion constant for soluble molecules in cell walls, may allow us to distinguish between these two possible types of signaling molecules, based on the biological time course of the CO_2 response, which shows measurable turgor-driven

stomatal conductance changes within 1–2 minutes of [CO₂]-shifts. CO₂ signal transduction events need to significantly precede such measurable stomatal conductance responses.

Ambient CO₂ concentration affects ethylene production in Arabidopsis leaves

To investigate whether ambient CO₂ concentrations affect ethylene production in Arabidopsis leaves, we exposed wild-type (Col-0), the ethylene synthesis mutants *acs* sextuple (*acs2-1;acs4-1;acs5-2;acs6-1;acs7-1;acs9-1*), *acs* septuple (*acs1-1;acs2-1;acs4-1;acs5-2;acs6-1;acs7-1;acs9-1*) and *acs* octuple (*acs2-1;acs4-1;acs5-2;acs6-1;acs7-1;acs9-1;amiR-acs8/acs11*) mutant plants to high (900 ppm) or low (150 ppm) [CO₂] for 90 min and quantified ethylene levels via gas-chromatography. Interestingly, ethylene levels in wild-type plants clearly and reproducibly increased upon exposure to 900 ppm [CO₂] compared to 150 ppm [CO₂] in more than three independent experimental sets, with slight variations between experiments (Figs 2, S1). Steady-state ethylene production was reduced in *acs* sextuple, septuple, and octuple mutant plants compared to wild-type (Figs 2, S1), similar to previous studies (Tsuchisaka *et al.*, 2009). Interestingly, ethylene levels were also elevated in response to high [CO₂] in sextuple and octuple mutant rosettes (Figs 2, S1). Yet, high [CO₂]-mediated ethylene levels in *acs* sextuple, septuple and octuple mutants reached only 51, 31, and 26% of WT levels, respectively (Fig. 2).

CO₂-mediated stomatal opening and closure are defective in *acs* octuple mutant plants

We measured stomatal conductance in response to [CO₂]-shifts in intact leaves of *acs* sextuple, septuple and octuple mutant plants to test whether defective ACC synthesis affects stomatal movements. Our results show intact stomatal conductance responses in leaves of *acs* sextuple and septuple mutant plants (Figs 3a–f, S2a–f). Interestingly, both high [CO₂]-induced stomatal closure and low [CO₂]-mediated stomatal opening were impaired in the leaves of *acs* octuple mutant plants compared to wild-type plants in independent sets of experiments (Figs 3g–i, S2g–i).

Leaves of the ethylene overproducer, *eto1-1*, show intact CO₂-induced stomatal conductance responses

To further investigate the involvement of ethylene in CO₂-mediated stomatal movements, we analyzed mutants in ethylene-signaling components for their CO₂-induced stomatal conductance responses. ETO1 is a negative regulator of ethylene biosynthesis. *eto1-1* mutant plants show constitutively activated ethylene signaling, increased ACS5 stability, and elevated ethylene production (Guzman & Ecker, 1990; Kieber *et al.*, 1993; Chae *et al.*, 2003). Analysis of ethylene production in *eto1-1* mutant plants showed a significant increase in response to high [CO₂] compared to low [CO₂] (Fig. 4a). Furthermore, at both CO₂ concentrations, *eto1-1* produced more ethylene than wild-type plants (P<0.05) in three independent experimental sets, yet its CO₂-mediated stomatal conductance responses to [CO₂]-shifts were robust and intact, comparable to wild-type (Figs 4b–d, S3).

Leaves of the ethylene-insensitive signaling mutants, *ein2-5* and *ein2-1*, show intact CO₂-induced stomatal conductance responses

EIN2 gene encodes a protein from the NRAMP family, a central positive regulator in the ethylene signaling pathway, which acts downstream to CTR1 (Alonso *et al.*, 1999; Ju *et al.*, 2012). To determine whether EIN2 is involved in CO₂-controlled stomatal movements, we analyzed two independent mutant alleles, *ein2-5* and *ein2-1* (Alonso *et al.*, 1999). Results showed robust and intact responses to [CO₂]-shifts of *ein2-5* mutant plants leaves, similar to wild-type (Fig 5a–c), in two independent labs (TAS and HK). However, in some of the experiments, the amplitudes of the stomatal responses of *ein2-1* mutant plants were slightly reduced compared to the wild-type (Figs 5d–f, S4).

CO₂-mediated stomatal movements are enhanced in leaves of ethylene receptor loss-of-function mutant plants

All five ethylene receptors function as negative regulators of ethylene signaling (Hua & Meyerowitz, 1998). The nature of mutations in these receptors can result in either a dominant gain-of-function (Bleecker *et al.*, 1988; Guzman & Ecker, 1990; Chang *et al.*, 1993; Wilkinson *et al.*, 1995), or a recessive loss-of-function receptor (Hua & Meyerowitz, 1998; Shakeel *et al.*, 2013). Combinatorial higher-order mutants of two or three recessive (loss-of-function) ethylene receptors results in a constitutive ethylene response phenotypes (Hua & Meyerowitz, 1998). First, we investigated whether a dominant gain-of-function mutation in ETR1 (Chang *et al.*, 1993) or ETR2 receptor (Sakai *et al.*, 1998) affects stomatal conductance in response to [CO₂]-shifts. Our investigation revealed intact CO₂-induced stomatal conductance responses in both the *etr1-1* and *etr2-1* (*etr1-1* Figs 6a–c, S5a–c; *etr2-1* Figs 6d–f, S5d–f).

Since gain-of-function mutants did not show an impaired phenotype, we analyzed stomatal movement responses of recessive loss-of-function single and higher-order ethylene receptor mutants. Interestingly, all loss-of-function mutant lines investigated here, including the triple mutant *etr2-3;ein4-4;ers2-3*, the double mutant *etr1-6;etr2-3* and the single mutants *etr1-6* showed enhanced stomatal opening in response to low [CO₂] (Figs 7, S6). The most pronounced phenotypes were observed in leaves of the triple mutant *etr2-3;ein4-4;ers2-3* and the double mutant *etr1-6;etr2-3*.

etr2-3;ein4-4;ers2-3 showed accelerated/enhanced stomatal opening in response to low [CO₂] (Fig. 7c (t4-t3) P=0.1), while the double mutant *etr1-6;etr2-3* and the single mutant, *etr1-6*, show both accelerated/enhanced stomatal opening (*etr1-6;etr2-3*: Fig. 7f (t4-t3) P=0.06, (t5-t3) P=0.02 ; *etr1-6*: Fig. 7l (t4-t3) P=0.02) in response to low [CO₂] and stomatal closing in response to high [CO₂] (*etr1-6;etr2-3*: Fig. 7f (t2-t1) P=0.02, (t3-t1) P=0.05 ; *etr1-6*: Fig. 7l (t2-t1) P=0.01). A prolonged gas-exchange analysis of the *etr1-6;etr2-3* to ambient, high, low, and then again high [CO₂] even further supports this dramatically enhanced stomatal response phenotype (Fig. S6c (t2-t1) P=0.001, (t6-t5) P=0.08). The accelerated/enhanced CO₂ responses shown here were obtained in three independent laboratories (UCSD USA, Newe Ya'ar Israel & Tartu Estonia) using either intact leaf or whole-plant gas-exchange systems, indicating the robustness of these CO₂ responses.

Impairment of ABA-induced stomatal movement responses in *acs* and ethylene receptor mutants.

Studies using stomatal aperture measurements in *Arabidopsis* have reported that ethylene either inhibits ABA-induced stomatal closing or stimulates stomatal closure (Tanaka *et al.*, 2005; Desikan *et al.*, 2006; She & Song, 2012; Chen *et al.*, 2013). To test whether a lack in ethylene biosynthesis or reception affects stomatal responses to ABA, we tested stomatal conductance responses to ABA in the ethylene biosynthesis *acs* octuple mutant and the above loss-of-function ethylene receptor mutants (triple mutant *etr2-3;ein4-4;ers2-3*, double mutant *etr1-6;etr2-3* and the single mutant *etr1-6*), which showed alternation in their stomatal conductance responses to CO₂.

We have used two different experimental settings in three different labs, where ABA was applied by xylem-sap feeding (Fig. 8) or by spraying intact plant rosettes (Fig. 9). In both types of experiments, wild-type leaves treated with ABA showed stomatal closure responses (Figs 8, 9). Treatment of *acs* octuple mutant leaves with ABA showed impaired stomatal closure responses (Fig. 8a–c, 8c (t3-t1) P=0.01; Fig. 9a–c, 9c (t3-t1) P=0.015). On the other hand, the ethylene-hypersensitive *etr1-6;etr2-3* showed an enhanced (rapid and stronger) stomatal closure in response to ABA (Fig. 8d–f, 8f (t2-t1) P=0.05, (t3-t1) P=0.09). Interestingly, while the triple mutant *etr2-3;ein4-4;ers2-3* showed wild-type stomatal closure (Fig. 9d–f), the double mutant *etr1-6;etr2-3* and the single mutant *etr1-6* showed an enhanced stomatal closure in response to ABA (*etr1-6;etr2-3* Fig. 8d–f, 8f (t2-t1) P=0.05, *etr1-6* Fig. 9g–i, 9i (t2-t1) P=0.016).

Discussion

In the present study, we pursued diffusion modeling to estimate whether a soluble or a gaseous molecule is more likely to diffuse from the mesophyll to guard cells as a rapid response to [CO₂]-shifts in intact plant leaves. Our model suggests that a gaseous signaling molecule with a shorter and more direct diffusion pathway to guard cells is more likely to be responsible for signaling rapid changes in stomatal conductance (Fig. 1). Previous research suggested that diffusion constants of soluble molecules through the cell wall space are 1–2 orders of magnitude smaller than in water (Kramer *et al.*, 2007). This indicates that a CO₂-triggered production of a soluble signal from mesophyll cells could result in considerable non-physiological delays in stomatal responses to changes in [CO₂]. The model presented here assumes that a mesophyll signal is not a steady-state amplifier of the response but that [CO₂] shifts trigger the production of the signal at the mesophyll cells (Sibbersen & Mott, 2010; Fujita *et al.*, 2013; Mott *et al.*, 2014). These simulations and previous research on other candidate gaseous molecules led us to investigate any potential effects of the gaseous phytohormone ethylene on CO₂-induced stomatal conductance regulation.

Our study reveals that ethylene biosynthesis is upregulated by elevated [CO₂] in wild-type *A. thaliana* leaves (Figs 2, S1), and is impaired in the higher-order *acs* mutants (sextuple, septuple, and octuple). The mechanism by which CO₂ mediates ethylene production has been previously studied (Abeles *et al.*, 1992; Mathooko, 1996) and found to include transcriptional, translational, and post-translational regulation of ACC synthase (ACS) (Mathooko *et al.*, 2001). Furthermore, the distinctive expression patterns and a combinatorial

interplay among the different ACS isoforms in *A. thaliana*, further increase the complexity and the role these genes play in regulating diverse developmental and physiological processes (Tsuchisaka & Theologis, 2004; Tsuchisaka *et al.*, 2009). The finding that exposure to elevated CO₂ caused clearly measurable macroscopic increases in ethylene production in intact rosettes indicates that one or more of the different cell types in leaves may contribute to the CO₂-induced ethylene increases. With the distinctive temporal and spatial expression patterns of the ACS genes (Tsuchisaka & Theologis, 2004; Datta *et al.*, 2015), further investigation is needed to determine the specific tissue/cells which produce and perceive ethylene in response to changes in [CO₂] and which of these tissues/cells are involved in CO₂-induced stomatal movements.

Many studies have provided evidence supporting a role for ethylene in stomatal aperture regulation in response to stimuli other than CO₂. However, the role of ethylene in these stomatal aperture responses were conducted in epidermal peels and showed ambiguous results. In some studies, ethylene was suggested to mediate stomatal opening (Levitt *et al.*, 1987; Iqbal *et al.*, 2011) via inhibition of ABA-induced stomatal closure (Tanaka *et al.*, 2005; Tanaka *et al.*, 2006; Wilkinson & Davies, 2009), and in others to induce stomatal closure (Desikan *et al.*, 2006; Zhang *et al.*, 2021). The experimental approaches using epidermal peels investigate signals that may depend on the state of guard cells and render time-resolved analyses more difficult. Notably, time-resolved stomatal conductance studies of intact leaves attached to intact plants and whole rosettes of intact plants have proven to aid in resolving the physiological responses of plants (McAusland *et al.*, 2016; Hiyama *et al.*, 2017; Ceciliato *et al.*, 2019), and circumvent limitations from the small sizes and the wide distribution of stomatal sizes in Arabidopsis. We, therefore, have based our experimental system on measurements of stomatal conductance kinetics in intact leaves. Combined measurements of ethylene production and time-resolved stomatal conductance recordings in response to [CO₂]-shifts of the different higher-order *acs* mutants revealed that only leaves of *acs* octuple mutant plants were significantly impaired in both high [CO₂]-induced stomatal closure and low [CO₂]-mediated stomatal opening (Figs 3g–i, S2g–i), while intact steady state and stomatal conductance responses to [CO₂]-shifts were observed in the ethylene over producer mutant *eto1-1* (Fig. 4). The significantly elevated ethylene levels in *eto1-1* plants in response to elevated [CO₂] indicate that additional ACC/ethylene production does not further enhance the stomatal response. This result, together with the observed impaired stomatal conductance response of the *acs* octuple mutant (Figs 3g–I, S2g–i), suggests that ethylene (above a minimum threshold) is a pre-requisite signal for intact stomatal conductance responses to [CO₂]. In this context, recent studies have shown direct roles of the ethylene precursor aminocyclopropane-1-carboxylic acid (ACC) as a signal molecule rather than just the precursor for ethylene (Yoon & Kieber, 2013; Van de Poel & Van Der Straeten, 2014; Mou *et al.*, 2020). Further research is needed to determine whether ACC participates as a signal in the stomatal CO₂ response.

To further investigate ethylene's role in stomatal conductance regulation, we conducted gas-exchange measurements of different ethylene signaling and reception mutants. EIN2 encodes the NRAMP-like protein ethylene insensitive 2, an early positive transducer of ethylene signaling that activates downstream transcriptional ethylene responses (Alonso *et al.*, 1999; Ju *et al.*, 2012; Qiao *et al.*, 2012). Interestingly, leaves of *ein2-5* and *ein2-1*

mutant plants showed robust and intact responses to [CO₂]-shifts (Figs 5, S4). We therefore chose to conduct our investigation on upstream components in the ethylene signaling pathway and analyzed different ethylene receptor mutants. Ethylene receptors function as negative regulators that suppress ethylene signaling. The dominant gain-of-function ethylene receptor *etr1-1* and *etr2-1* mutants have been shown to lead to ethylene-insensitivity (Chang *et al.*, 1993; Hua *et al.*, 1995). Remarkably, our data show that CO₂-mediated stomatal conductance responses in intact plant leaves of these mutants were wildtype-like (Fig. 6). On the other hand, ETR1, ETR2, EIN4, and ERS ethylene receptor loss-of-function mutants are characterized by constitutive/hypersensitive ethylene responses, which found to be more pronounced in higher-order mutant lines (Hua & Meyerowitz, 1998; Cancel & Larsen, 2002; Qu *et al.*, 2007). This observation underline the partial over-lapping redundant function of the different ethylene receptors in ethylene signaling (Theologis, 1998). Indeed, in our investigation, all studied loss-of-function receptor mutants, *etr2-3;ein4-4;ers2-3*, *etr1-6;etr2-3* and *etr1-6* showed enhanced/accelerated stomatal conductance responses to [CO₂], while the higher-order *etr2-3;ein4-4;ers2-3* triple mutant, and *etr1-6;etr2-3* double mutant showed the most pronounced enhanced CO₂ response phenotypes. Interestingly, lines that included the loss-of-function mutation in ETR1 (i.e., *etr1-6;etr2-3* and *etr1-6*) showed a distinctive phenotype of an enhanced/accelerated response to both low [CO₂] induce stomatal opening and high [CO₂] induced stomatal closure (Figs 7d-f, g-i, S6). The observed intact stomatal conductance responses to [CO₂] in the ethylene insensitive single mutants and enhanced/accelerated responses of the ethylene hypersensitive loss-of-function receptor mutants, can be explained by the high redundancy of ethylene receptors in Arabidopsis. On the other hand, different studies have suggested that ethylene receptors may have ethylene-independent roles (Beaudoin *et al.*, 2000; Desikan *et al.*, 2005; Binder *et al.*, 2006; Wilson *et al.*, 2014; Bakshi *et al.*, 2015; Bakshi *et al.*, 2018), which may be involved in the accelerated stomatal responses revealed here. In the last few years, in-depth research into ethylene receptor functions has revealed their roles in non-canonical signal transduction pathways, which do not signal via the well-known CTR1/EIN2 signaling cascade (Kieber *et al.*, 1993; Binder, 2020). The present findings that loss-of-function *etr1-6;etr2-3* mutant plants significantly accelerate stomatal responses to [CO₂], while stomatal conductance responses in *ein2-1* and *ein2-5* are intact, may be explained by the recently recognized additional roles of the ETR1 and ETR2 in non-canonical plant signaling (Wilson *et al.*, 2014; Bakshi *et al.*, 2018; Piya *et al.*, 2019; Binder, 2020). Further research is needed to distinguish and dissect between this canonical/non-canonical and ethylene dependent/independent signaling pathways.

Abscisic acid (ABA) is one of the key hormones involved in stomatal conductance regulation. A crosstalk between ABA and ethylene signaling has been previously suggested, yet the outcome of ABA and ethylene interaction in regulating stomatal apertures has remained controversial (see references above). The present study reveals a correlation between altered stomatal conductance phenotypes in *acs* octuple and *etr1-6* mutants to [CO₂] and ABA. *acs* octuple mutant plants showed an impaired stomatal opening and closure to low/high CO₂ and a significantly impaired stomatal closure to ABA. On the other hand, a significant enhanced/accelerated stomatal opening and closure in response to low/high CO₂ was found in both the *etr1-6;etr2-3* double mutant, and *etr1-6* single mutant plants,

which also showed an enhanced response to ABA. These contrasting phenotypes between the ethylene biosynthesis mutant and the hypersensitive loss-of-function receptor mutant further support a model in which CO₂ and ABA signaling pathways merge downstream of early sensing and signaling mechanisms and influence one another (Raschke, 1975; Chater *et al.*, 2015; Hsu *et al.*, 2018)

Ethylene receptors involve in various signaling and developmental processes (Iqbal *et al.*, 2017; Khan *et al.*, 2017). The *etr1-6* loss-of-function ethylene receptor mutant showed hypersensitive response to ABA induced-stomatal closure in this study. On the other hand, in seed germination studies, the *etr1-6* mutant showed an insensitive response to ABA and germinated faster (Bakshi *et al.*, 2018). Ethylene reception and signaling are substantially more complex than assumed. The different ethylene receptors form homodimers (Schaller & Bleecker, 1995; Schaller *et al.*, 1995) and heterodimers (Gao *et al.*, 2008; Grefen *et al.*, 2008; Gao & Schaller, 2009). In addition, the different ethylene receptors were expressed differently in various plant tissues and at diverse developmental stages (Grefen *et al.*, 2008). The regulation of ethylene biosynthesis also differs between tissues (Mathooko, 1996). For example, high [CO₂] induces ethylene biosynthesis in leaves (Grodzinski *et al.*, 1982; Kao & Yang, 1982; Philosoph-Hadas *et al.*, 1986), while in fruit, high [CO₂] inhibits ethylene production (Cheverry *et al.*, 1988; Oetiker & Yang, 1995). Together, these features add complexity to ethylene perception and signal transduction and to the role each of the ethylene receptors plays in the different tissues (for example, seeds/guard cells).

Different studies have investigated crosstalk between ethylene and ABA in stomatal conductance regulation (Wilkinson & Davies, 2010; Muller, 2021). Ethylene has been found to induce components of the ABA biosynthesis pathway, as ABA levels were altered in response to impairment in ethylene reception (*etr1-2*) (Chiwocha *et al.*, 2005) or biosynthesis (*acs7*) (Dong *et al.*, 2011). Furthermore, Bakshi *et al.* (2018) suggested the involvement of the ETR1 receiver domain in the induction of ABA signaling genes by ABA. This finding supports a role for ETR1 in ABA signaling via a non-canonical signaling pathway (independent of CTR1). Thus, effects of ethylene receptor mutants on ABA responses in different tissues are of interest.

Enhancing the rate (“speed”) of stomatal responses has been suggested as an avenue for increasing plant photosynthetic and water-use-efficiency during fluctuating light conditions, with stomatal responses in part being driven by CO₂ concentration changes in leaves (Taylor & Long, 2017; Lawson & Vialet-Chabrand, 2019). The present study has identified a role of ethylene receptors in modulating the rate of stomatal conductance changes to [CO₂] and abscisic acid. Further insights into the mechanisms mediating accelerated stomatal responses in ethylene receptor loss-of-function mutants could provide an avenue for engineering improved water-use-efficiency and stomatal performance of plants.

In summary, we show that elevated [CO₂] induces an increase in ethylene production in intact wild-type *A. thaliana* rosettes. Furthermore, higher-order ethylene biosynthesis *acs* octuple mutant plants show impaired stomatal conductance responses to high and low [CO₂]. Consistent with a role for ethylene component signaling, loss-of-function ethylene receptor mutant plants in the negatively regulating ethylene receptors amplify/

accelerate CO₂-regulated stomatal movements. Furthermore, the loss-of-function receptor mutant *etr1-6* enhances/accelerates [CO₂] and ABA-controlled stomatal movements, further supporting a model in which CO₂ and ABA signaling pathways merge downstream of receptors and sensing mechanisms and influence one-another. The accelerated stomatal responses in ethylene receptor mutants found here are of interest for efforts aimed at increasing the rate of stomata movement kinetics for enhanced plant performance. Whether the presently described CO₂ responses are due to functions of the mutated ACC synthase and ethylene receptor genes in leaf mesophyll, guard cells, or other tissues requires future investigations.

Supplementary Material

Refer to Web version on PubMed Central for supplementary material.

Acknowledgements

We thank Sakis Theologis, Brad Binder, Jose Alonso, and Joseph Ecker for providing ethylene synthesis and response mutants for the present study. We thank Caren Chang for scientific feedback and discussions. This research was funded by a grant from the National Science Foundation (MCB-1900567) to JIS and W.-J.R., by the Israel Science Foundation (grant No. 768/20) to T.A.S and in part by NIH grant R01GM060396 to J.I.S. S.S. was in part supported by a DFG postdoctoral fellowship (SCHU 3186/1-1:1). This research was in part supported by the Estonian Research Council (PRG433) and European Regional Development Fund (Center of Excellence in Molecular Cell Engineering CEMCE) to HK.

Data Availability

The data that support the findings of this study is included and available as supporting information (Dataset S1). Mutant seed stocks are either publicly available when indicated or will be provided upon request.

References

- Abeles FB, Morgan PW, Saltveit ME. 1992. Ethylene in plant biology. San Diego: Academic Press.
- Alonso JM, Hirayama T, Roman G, Nourizadeh S, Ecker JR. 1999. EIN2, a bifunctional transducer of ethylene and stress responses in Arabidopsis. *Science* 284(5423): 2148–2152. [PubMed: 10381874]
- Assmann SM, Jegla T. 2016. Guard cell sensory systems: recent insights on stomatal responses to light, abscisic acid, and CO₂. *Current Opinion in Plant Biology* 33: 157–167. [PubMed: 27518594]
- Astrath NG, Shen J, Song D, Rohling JH, Astrath FB, Zhou J, Navessin T, Liu ZS, Gu CE, Zhao X. 2009. The effect of relative humidity on binary gas diffusion. *J Phys Chem B* 113(24): 8369–8374. [PubMed: 19514781]
- Lindsey Iii BE, Rivero L, Calhoun CS, Grotewold E, Brkljacic J. 2017. Standardized Method for High-throughput Sterilization of Arabidopsis Seeds. *JoVE*(128): e56587.
- Bakshi A, Piya S, Fernandez JC, Chervin C, Hewezi T, Binder BM. 2018. Ethylene Receptors Signal via a Noncanonical Pathway to Regulate Abscisic Acid Responses. *Plant Physiology* 176(1): 910–929. [PubMed: 29158332]
- Bakshi A, Wilson RL, Lacey RF, Kim H, Wuppalapati SK, Binder BM. 2015. Identification of Regions in the Receiver Domain of the ETHYLENE RESPONSE1 Ethylene Receptor of Arabidopsis Important for Functional Divergence. *Plant Physiology* 169(1): 219–232. [PubMed: 26160962]
- Beaudoin N, Serizet C, Gosti F, Giraudat J. 2000. Interactions between abscisic acid and ethylene signaling cascades. *PLANT CELL* 12(7): 1103–1115. [PubMed: 10899977]

- Binder BM. 2020. Ethylene signaling in plants. *Journal of Biological Chemistry* 295(22): 7710–7725. [PubMed: 32332098]
- Binder BM, O'Malley RC, Wang W, Zutz TC, Bleecker AB. 2006. Ethylene stimulates nutations that are dependent on the ETR1 receptor. *Plant Physiology* 142(4): 1690–1700. [PubMed: 17071649]
- Bleecker AB, Estelle MA, Somerville C, Kende H. 1988. Insensitivity to Ethylene Conferred by a Dominant Mutation in *Arabidopsis thaliana*. *Science* 241(4869): 1086–1089. [PubMed: 17747490]
- Busch FA, Holloway-Phillips M, Stuart-Williams H, Farquhar GD. 2020. Revisiting carbon isotope discrimination in C3 plants shows respiration rules when photosynthesis is low. *Nature Plants* 6(3): 245–258. [PubMed: 32170287]
- Cancel JD, Larsen PB. 2002. Loss-of-Function Mutations in the Ethylene Receptor ETR1 Cause Enhanced Sensitivity and Exaggerated Response to Ethylene in *Arabidopsis*. *Plant Physiology* 129(4): 1557–1567. [PubMed: 12177468]
- Ceciliato PHO, Zhang J, Liu Q, Shen X, Hu H, Liu C, Schäffner AR, Schroeder JI. 2019. Intact leaf gas exchange provides a robust method for measuring the kinetics of stomatal conductance responses to abscisic acid and other small molecules in *Arabidopsis* and grasses. *Plant Methods* 15(1): 38. [PubMed: 31019545]
- Chae HS, Faure F, Kieber JJ. 2003. The *eto1*, *eto2*, and *eto3* mutations and cytokinin treatment increase ethylene biosynthesis in *Arabidopsis* by increasing the stability of ACS protein. *PLANT CELL* 15(2): 545–559. [PubMed: 12566591]
- Chandrasekhar S 1943. Stochastic problems in physics and astronomy. *Reviews of Modern Physics* 15(1): 0001–0089.
- Chang C, Kwok SF, Bleecker AB, Meyerowitz EM. 1993. *Arabidopsis* ethylene-response gene ETR1: similarity of product to two-component regulators. *Science* 262(5133): 539–544. [PubMed: 8211181]
- Chater C, Peng K, Movahedi M, Dunn JA, Walker HJ, Liang YK, McLachlan DH, Casson S, Isner JC, Wilson I, et al. 2015. Elevated CO₂-Induced Responses in Stomata Require ABA and ABA Signaling. *Current Biology* 25(20): 2709–2716. [PubMed: 26455301]
- Chaves AR, Tomas JO. 1984. Effect of a Brief CO₂ Exposure on Ethylene Production. *Plant Physiology* 76(1): 88–91. [PubMed: 16663830]
- Chen L, Dodd IC, Davies WJ, Wilkinson S. 2013. Ethylene limits abscisic acid- or soil drying-induced stomatal closure in aged wheat leaves. *Plant Cell Environ* 36(10): 1850–1859. [PubMed: 23488478]
- Chen W, Levine H, Rappel WJ. 2009. Compartmentalization of second messengers in neurons: a mathematical analysis. *Phys Rev E Stat Nonlin Soft Matter Phys* 80(4 Pt 1): 041901. [PubMed: 19905336]
- Chevrey JL, Sy MO, Pouliquen J, Marcellin P. 1988. Regulation by CO₂ of 1-aminocyclopropane-1-carboxylic acid conversion to ethylene in climacteric fruits. *Physiologia plantarum* 72(3): 535–540.
- Chiwocha SD, Cutler AJ, Abrams SR, Ambrose SJ, Yang J, Ross AR, Kermod AR. 2005. The *etr1-2* mutation in *Arabidopsis thaliana* affects the abscisic acid, auxin, cytokinin and gibberellin metabolic pathways during maintenance of seed dormancy, moist-chilling and germination. *Plant J* 42(1): 35–48. [PubMed: 15773852]
- Clark KL, Larsen PB, Wang X, Chang C. 1998. Association of the *Arabidopsis* CTR1 Raf-like kinase with the ETR1 and ERS ethylene receptors. *Proc Natl Acad Sci U S A* 95(9): 5401–5406. [PubMed: 9560288]
- Daeter W, Hartung W. 1993. The permeability of the epidermal cell plasma membrane of barley leaves to abscisic acid. *Planta* 191(1): 41–47.
- Daszkowska-Golec A, Szarejko I. 2013. Open or close the gate - stomata action under the control of phytohormones in drought stress conditions. *Front Plant Sci* 4: 138. [PubMed: 23717320]
- Datta R, Kumar D, Sultana A, Hazra S, Bhattacharyya D, Chattopadhyay S. 2015. Glutathione Regulates 1-Aminocyclopropane-1-Carboxylate Synthase Transcription via WRKY33 and 1-Aminocyclopropane-1-Carboxylate Oxidase by Modulating Messenger RNA Stability to Induce Ethylene Synthesis during Stress. *Plant Physiology* 169(4): 2963–2981. [PubMed: 26463088]

- Desikan R, Last K, Hancock J, Hooley R, Neill S. 2005. Role of ETR1 in ethylene and hydrogen peroxide signalling in guard cells. *Comparative Biochemistry and Physiology a-Molecular & Integrative Physiology* 141(3): S307–S307.
- Desikan R, Last K, Harrett-Williams R, Tagliavia C, Harter K, Hooley R, Hancock JT, Neill SJ. 2006. Ethylene-induced stomatal closure in Arabidopsis occurs via AtrbohF-mediated hydrogen peroxide synthesis. *Plant Journal* 47(6): 907–916.
- Dodd I 2003. Hormonal Interactions and Stomatal Responses. *Journal of Plant Growth Regulation* 22(1): 32–46.
- Dong H, Zhen Z, Peng J, Chang L, Gong Q, Wang NN. 2011. Loss of ACS7 confers abiotic stress tolerance by modulating ABA sensitivity and accumulation in Arabidopsis. *Journal of experimental botany* 62(14): 4875–4887. [PubMed: 21765163]
- Else MA, Tiekstra AE, Croker SJ, Davies WJ, Jackson MB. 1996. Stomatal Closure in Flooded Tomato Plants Involves Abscisic Acid and a Chemically Unidentified Anti-Transpirant in Xylem Sap. *Plant Physiology* 112(1): 239–247. [PubMed: 12226387]
- Farquhar GD, Caemmerer SV, Berry JA. 1980. A Biochemical-Model of Photosynthetic Co2 Assimilation in Leaves of C-3 Species. *Planta* 149(1): 78–90. [PubMed: 24306196]
- Fernandez-Maculet JC, Dong JG, Yang SF. 1993. Activation of 1-aminocyclopropane-1-carboxylate oxidase by carbon dioxide. *Biochem Biophys Res Commun* 193(3): 1168–1173. [PubMed: 8391802]
- Flütsch S, Nigro A, Conci F, Fajkus J, Thalmann M, Trtíflek M, Panzarová K, Santelia D. 2020. Glucose uptake to guard cells via STP transporters provides carbon sources for stomatal opening and plant growth. *EMBO reports* 21(8): e49719. [PubMed: 32627357]
- Fujita T, Noguchi K, Ozaki H, Terashima I. 2019. Confirmation of mesophyll signals controlling stomatal responses by a newly devised transplanting method. *Funct Plant Biol* 46(5): 467–481. [PubMed: 30940335]
- Fujita T, Noguchi K, Terashima I. 2013. Apoplastic mesophyll signals induce rapid stomatal responses to CO2 in *Commelina communis*. *New Phytol* 199(2): 395–406. [PubMed: 23560389]
- Gallie DR. 2015. Ethylene receptors in plants - why so much complexity? *F1000Prime Rep* 7: 39. [PubMed: 26171216]
- Gao Z, Chen YF, Randlett MD, Zhao XC, Findell JL, Kieber JJ, Schaller GE. 2003. Localization of the Raf-like kinase CTR1 to the endoplasmic reticulum of Arabidopsis through participation in ethylene receptor signaling complexes. *J Biol Chem* 278(36): 34725–34732. [PubMed: 12821658]
- Gao Z, Schaller GE. 2009. The role of receptor interactions in regulating ethylene signal transduction. *Plant Signal Behav* 4(12): 1152–1153. [PubMed: 20514232]
- Gao Z, Wen CK, Binder BM, Chen YF, Chang J, Chiang YH, Kerris RJ 3rd, Chang C, Schaller GE. 2008. Heteromeric interactions among ethylene receptors mediate signaling in Arabidopsis. *J Biol Chem* 283(35): 23801–23810. [PubMed: 18577522]
- Geng S, Misra BB, de Armas E, Huhman DV, Alborn HT, Sumner LW, Chen S. 2016. Jasmonate-mediated stomatal closure under elevated CO2 revealed by time-resolved metabolomics. *Plant J*.
- Gorny JR, Kader AA. 1996. Controlled-atmosphere Suppression of ACC Synthase and ACC Oxidase in 'Golden Delicious' Apples during Long-term Cold Storage. *Journal of the American Society for Horticultural Science* 121(4): 751–755.
- Grefen C, Stadele K, Ruzicka K, Obrdlik P, Harter K, Horak J. 2008. Subcellular localization and in vivo interactions of the Arabidopsis thaliana ethylene receptor family members. *Mol Plant* 1(2): 308–320. [PubMed: 19825542]
- Grodzinski B, Boesel I, Horton RF. 1982. Ethylene Release from Leaves of *Xanthium strumarium* L. and *Zea mays* L. *Journal of experimental botany* 33(2): 344–354.
- Guzman P, Ecker JR. 1990. Exploiting the triple response of Arabidopsis to identify ethylene-related mutants. *PLANT CELL* 2(6): 513–523. [PubMed: 2152173]
- Hanstein SM, Felle HH. 2002. CO2-triggered chloride release from guard cells in intact fava bean leaves. Kinetics of the onset of stomatal closure. *Plant Physiology* 130(2): 940–950. [PubMed: 12376658]
- Haynes WM, Lide DR, & Bruno TJ . 2016. CRC handbook of chemistry and physics: a ready-reference book of chemical and physical data. Boca Raton, Florida: CRC Press.

- Hetherington AM, Woodward FI. 2003. The role of stomata in sensing and driving environmental change. *Nature* 424(6951): 901–908. [PubMed: 12931178]
- Hiyama A, Takemiya A, Munemasa S, Okuma E, Sugiyama N, Tada Y, Murata Y, Shimazaki K-i. 2017. Blue light and CO₂ signals converge to regulate light-induced stomatal opening. *Nature Communications* 8(1): 1284.
- Hsu PK, Takahashi Y, Munemasa S, Merilo E, Laanemets K, Waadt R, Pater D, Kollist H, Schroeder JI. 2018. Abscisic acid-independent stomatal CO₂ signal transduction pathway and convergence of CO₂ and ABA signaling downstream of OST1 kinase. *Proc Natl Acad Sci U S A* 115(42): E9971–E9980. [PubMed: 30282744]
- Hua J, Chang C, Sun Q, Meyerowitz E. 1995. Ethylene insensitivity conferred by Arabidopsis ERS gene. *Science* 269(5231): 1712–1714. [PubMed: 7569898]
- Hua J, Meyerowitz EM. 1998. Ethylene responses are negatively regulated by a receptor gene family in Arabidopsis thaliana. *Cell* 94(2): 261–271. [PubMed: 9695954]
- Iqbal N, Khan NA, Ferrante A, Trivellini A, Francini A, Khan MIR. 2017. Ethylene Role in Plant Growth, Development and Senescence: Interaction with Other Phytohormones. *Frontiers in Plant Science* 8.
- Iqbal N, Nazar R, Syeed S, Masood A, Khan NA. 2011. Exogenously-sourced ethylene increases stomatal conductance, photosynthesis, and growth under optimal and deficient nitrogen fertilization in mustard. *Journal of experimental botany* 62(14): 4955–4963. [PubMed: 21705383]
- Ju C, Yoon GM, Shemansky JM, Lin DY, Ying ZI, Chang J, Garrett WM, Kessenbrock M, Groth G, Tucker ML, et al. 2012. CTR1 phosphorylates the central regulator EIN2 to control ethylene hormone signaling from the ER membrane to the nucleus in Arabidopsis. *Proc Natl Acad Sci U S A* 109(47): 19486–19491. [PubMed: 23132950]
- Kao CH, Yang SF. 1982. Light inhibition of the conversion of 1-aminocyclopropane-1-carboxylic acid to ethylene in leaves is mediated through carbon dioxide. *Planta* 155(3): 261–266. [PubMed: 24271776]
- Khan NA, Khan MIR, Ferrante A, Poor P. 2017. Editorial: Ethylene: A Key Regulatory Molecule in Plants. *Frontiers in Plant Science* 8.
- Kieber JJ, Rothenberg M, Roman G, Feldmann KA, Ecker JR. 1993. CTR1, a negative regulator of the ethylene response pathway in Arabidopsis, encodes a member of the raf family of protein kinases. *Cell* 72(3): 427–441. [PubMed: 8431946]
- Kim H, Helmbrecht EE, Stalans MB, Schmitt C, Patel N, Wen CK, Wang W, Binder BM. 2011. Ethylene receptor ETHYLENE RECEPTOR1 domain requirements for ethylene responses in Arabidopsis seedlings. *Plant Physiology* 156(1): 417–429. [PubMed: 21386032]
- Kim TH, Bohmer M, Hu H, Nishimura N, Schroeder JI. 2010. Guard cell signal transduction network: advances in understanding abscisic acid, CO₂, and Ca²⁺ signaling. *Annual Review of Plant Biology*. 61: 561–591.
- Kolla VA, Vavasseur A, Raghavendra AS. 2007. Hydrogen peroxide production is an early event during bicarbonate induced stomatal closure in abaxial epidermis of Arabidopsis. *Planta* 225(6): 1421–1429. [PubMed: 17160388]
- Kollist H, Nuhkat M, Roelfsema MRG. 2014. Closing gaps: linking elements that control stomatal movement. *New Phytologist* 203(1): 44–62. [PubMed: 24800691]
- Kollist T, Moldau H, Rasulov B, Oja V, Rämme H, Hüve K, Jaspers P, Kangasjärvi J, Kollist H. 2007. A novel device detects a rapid ozone-induced transient stomatal closure in intact Arabidopsis and its absence in abi2 mutant. *Physiologia plantarum* 129(4): 796–803.
- Kramer EM, Frazer NL, Baskin TI. 2007. Measurement of diffusion within the cell wall in living roots of Arabidopsis thaliana. *Journal of experimental botany* 58(11): 3005–3015. [PubMed: 17728296]
- Lawson T, Lefebvre S, Baker NR, Morison JI, Raines CA. 2008. Reductions in mesophyll and guard cell photosynthesis impact on the control of stomatal responses to light and CO₂. *Journal of experimental botany* 59(13): 3609–3619. [PubMed: 18836187]
- Lawson T, Viallet-Chabrand S. 2019. Speedy stomata, photosynthesis and plant water use efficiency. *New Phytologist* 221(1): 93–98. [PubMed: 29987878]
- Lee J, Bowling DJF. 1992. Effect of the Mesophyll on Stomatal Opening in Commelina-Communis. *Journal of experimental botany* 43(252): 951–957.

- Lee JS, Bowling DJF. 1995. Influence of the Mesophyll on Stomatal Opening. *Australian Journal of Plant Physiology* 22(3): 357–363.
- Levitt LK, Stein DB, Rubinstein B. 1987. Promotion of Stomatal Opening by Indoleacetic Acid and Ethrel in Epidermal Strips of *Vicia faba* L. *Plant Physiology* 85(2): 318–321. [PubMed: 16665694]
- Mathooko FM. 1996. Regulation of ethylene biosynthesis in higher plants by carbon dioxide. *Postharvest Biology and Technology* 7(1–2): 1–26.
- Mathooko FM, Mwaniki MW, Nakatsuka A, Shiomi S, Kubo Y, Inaba A, Nakamura R 1999. Expression characteristics of CS-ACS1, CS-ACS2 and CS-ACS3, three members of the 1-aminocyclopropane-1-carboxylate synthase gene family in cucumber (*Cucumis sativus* L.) fruit under carbon dioxide stress. 164–164–172.
- Mathooko FM, Tsunashima Y, Owino WZO, Kubo Y, Inaba A. 2001. Regulation of genes encoding ethylene biosynthetic enzymes in peach (*Prunus persica* L.) fruit by carbon dioxide and 1-methylcyclopropene. *Postharvest Biology and Technology* 21(3): 265–281.
- McAusland L, Vialet-Chabrand S, Davey P, Baker NR, Brendel O, Lawson T. 2016. Effects of kinetics of light-induced stomatal responses on photosynthesis and water-use efficiency. *New Phytologist* 211(4): 1209–1220. [PubMed: 27214387]
- Mott KA. 1988. Do stomata respond to CO₂ concentrations other than intercellular? *Plant Physiology* 86(1): 200–203. [PubMed: 16665866]
- Mott KA. 2009. Opinion: Stomatal responses to light and CO₂ depend on the mesophyll. *Plant Cell and Environment* 32(11): 1479–1486.
- Mott KA, Berg DG, Hunt SM, Peak D. 2014. Is the signal from the mesophyll to the guard cells a vapour-phase ion? *Plant Cell Environ* 37(5): 1184–1191. [PubMed: 24313673]
- Mou W, Kao YT, Michard E, Simon AA, Li D, Wudick MM, Lizzio MA, Feijo JA, Chang C. 2020. Ethylene-independent signaling by the ethylene precursor ACC in *Arabidopsis* ovular pollen tube attraction. *Nat Commun* 11(1): 4082. [PubMed: 32796832]
- Muller M 2021. Foes or Friends: ABA and Ethylene Interaction under Abiotic Stress. *Plants (Basel)* 10(3): 448. [PubMed: 33673518]
- Murata Y, Mori IC, Munemasa S. 2015. Diverse stomatal signaling and the signal integration mechanism. *Annu Rev Plant Biol* 66: 369–392. [PubMed: 25665132]
- Oetiker JH, Yang SF 1995. THE ROLE OF ETHYLENE IN FRUIT RIPENING: International Society for Horticultural Science (ISHS), Leuven, Belgium. 167–178.
- Pattyn J, Vaughan-Hirsch J, Van de Poel B. 2021. The regulation of ethylene biosynthesis: a complex multilevel control circuitry. *New Phytol* 229(2): 770–782. [PubMed: 32790878]
- Philosoph-Hadas S, Aharoni N, Yang SF. 1986. Carbon dioxide enhances the development of the ethylene forming enzyme in tobacco leaf discs. *Plant Physiology* 82(4): 925–929. [PubMed: 16665167]
- Piya S, Binder BM, Hewezi T. 2019. Canonical and noncanonical ethylene signaling pathways that regulate *Arabidopsis* susceptibility to the cyst nematode *Heterodera schachtii*. *New Phytol* 221(2): 946–959. [PubMed: 30136723]
- Pospíšilová J 2003. Participation of Phytohormones in the Stomatal Regulation of Gas Exchange During Water Stress. *Biologia Plantarum* 46(4): 491–506.
- Pritchard DT, Currie JA. 1982. Diffusion of coefficients of carbon dioxide, nitrous oxide, ethylene and ethane in air and their measurement. *Journal of Soil Science* 33(2): 175–184.
- Qiao H, Shen Z, Huang SS, Schmitz RJ, Urich MA, Briggs SP, Ecker JR. 2012. Processing and subcellular trafficking of ER-tethered EIN2 control response to ethylene gas. *Science* 338(6105): 390–393. [PubMed: 22936567]
- Qu X, Hall BP, Gao Z, Schaller GE. 2007. A strong constitutive ethylene-response phenotype conferred on *Arabidopsis* plants containing null mutations in the ethylene receptors ETR1 and ERS1. *BMC Plant Biology* 7(1): 3. [PubMed: 17224067]
- Raschke K 1975. Simultaneous requirement of carbon dioxide and abscisic acid for stomatal closing in *Xanthium strumarium* L. *Planta* 125(3): 243–259. [PubMed: 24435438]
- Sakai H, Hua J, Chen QG, Chang C, Medrano LJ, Bleecker AB, Meyerowitz EM. 1998. ETR2 is an ETR1-like gene involved in ethylene signaling in *Arabidopsis*. *Proc Natl Acad Sci U S A* 95(10): 5812–5817. [PubMed: 9576967]

- Schaller GE, Bleecker AB. 1995. Ethylene-binding sites generated in yeast expressing the Arabidopsis ETR1 gene. *Science* 270(5243): 1809–1811. [PubMed: 8525372]
- Schaller GE, Ladd AN, Lanahan MB, Spanbauer JM, Bleecker AB. 1995. The ethylene response mediator ETR1 from Arabidopsis forms a disulfide-linked dimer. *J Biol Chem* 270(21): 12526–12530. [PubMed: 7759498]
- Schmelz EA, Engelberth J, Alborn HT, O'Donnell P, Sammons M, Toshima H, Tumlinson JH. 2003. Simultaneous analysis of phytohormones, phytotoxins, and volatile organic compounds in plants. *Proceedings of the National Academy of Sciences of the United States of America* 100(18): 10552–10557. [PubMed: 12874387]
- Shakeel SN, Wang X, Binder BM, Schaller GE. 2013. Mechanisms of signal transduction by ethylene: overlapping and non-overlapping signalling roles in a receptor family. *AoB PLANTS* 5.
- She X, Song X. 2012. Ethylene inhibits abscisic acid-induced stomatal closure in *Vicia faba* via reducing nitric oxide levels in guard cells. *New Zealand Journal of Botany* 50(2): 203–216.
- Sibbersen E, Mott KA. 2010. Stomatal Responses to Flooding of the Intercellular Air Spaces Suggest a Vapor-Phase Signal Between the Mesophyll and the Guard Cells. *Plant Physiology* 153(3): 1435–1442. [PubMed: 20472750]
- Tanaka Y, Sano T, Tamaoki M, Nakajima N, Kondo N, Hasezawa S. 2005. Ethylene inhibits abscisic acid-induced stomatal closure in Arabidopsis. *Plant Physiology* 138(4): 2337–2343. [PubMed: 16024687]
- Tanaka Y, Sano T, Tamaoki M, Nakajima N, Kondo N, Hasezawa S. 2006. Cytokinin and auxin inhibit abscisic acid-induced stomatal closure by enhancing ethylene production in Arabidopsis. *Journal of experimental botany* 57(10): 2259–2266. [PubMed: 16798847]
- Taylor SH, Long SP. 2017. Slow induction of photosynthesis on shade to sun transitions in wheat may cost at least 21% of productivity. *Philosophical Transactions of the Royal Society B: Biological Sciences* 372(1730): 20160543.
- Theologis A. 1998. Ethylene signalling: redundant receptors all have their say. *Current Biology* 8(24): R875–878. [PubMed: 9843677]
- Tsuchisaka A, Theologis A. 2004. Unique and overlapping expression patterns among the arabidopsis 1-amino-cyclopropane-1-carboxylate synthase gene family members. *Plant Physiology* 136(2): 2982–3000. [PubMed: 15466221]
- Tsuchisaka A, Yu G, Jin H, Alonso JM, Ecker JR, Zhang X, Gao S, Theologis A. 2009. A combinatorial interplay among the 1-aminocyclopropane-1-carboxylate isoforms regulates ethylene biosynthesis in Arabidopsis thaliana. *Genetics* 183(3): 979–1003. [PubMed: 19752216]
- Van de Poel B, Van Der Straeten D. 2014. 1-aminocyclopropane-1-carboxylic acid (ACC) in plants: more than just the precursor of ethylene! *Frontiers in Plant Science* 5(640).
- Wang KL, Li H, Ecker JR. 2002. Ethylene biosynthesis and signaling networks. *PLANT CELL* 14 Suppl: S131–151. [PubMed: 12045274]
- Wen X, Zhang C, Ji Y, Zhao Q, He W, An F, Jiang L, Guo H. 2012. Activation of ethylene signaling is mediated by nuclear translocation of the cleaved EIN2 carboxyl terminus. *Cell Res* 22(11): 1613–1616. [PubMed: 23070300]
- Wheeler J, Levreault R. 1985. The peculiar Type I supernova in NGC 991. *The Astrophysical Journal* 294: L17–L20.
- Wilkinson JQ, Lanahan MB, Yen HC, Giovannoni JJ, Klee HJ. 1995. An ethylene-inducible component of signal transduction encoded by never-ripe. *Science* 270(5243): 1807–1809. [PubMed: 8525371]
- Wilkinson S, Davies WJ. 2009. Ozone suppresses soil drying- and abscisic acid (ABA)-induced stomatal closure via an ethylene-dependent mechanism. *Plant Cell Environ* 32(8): 949–959. [PubMed: 19302171]
- Wilkinson S, Davies WJ. 2010. Drought, ozone, ABA and ethylene: new insights from cell to plant to community. *Plant, cell & environment* 33(4): 510–525.
- Wilson RL, Kim H, Bakshi A, Binder BM. 2014. The Ethylene Receptors ETHYLENE RESPONSE1 and ETHYLENE RESPONSE2 Have Contrasting Roles in Seed Germination of Arabidopsis during Salt Stress. *Plant Physiology* 165(3): 1353–1366. [PubMed: 24820022]

- Winn EB. 1950. The Temperature Dependence of the Self-Diffusion Coefficients of Argon, Neon, Nitrogen, Oxygen, Carbon Dioxide, and Methane. *Physical Review* 80(6): 1024–1027.
- Wong SC, Cowan IR, Farquhar GD. 1979. Stomatal conductance correlates with photosynthetic capacity. *Nature* 282(5737): 424–426.
- Wuyts N, Palauqui JC, Conejero G, Verdeil JL, Granier C, Massonnet C. 2010. High-contrast three-dimensional imaging of the Arabidopsis leaf enables the analysis of cell dimensions in the epidermis and mesophyll. *Plant Methods* 6: 17. [PubMed: 20598116]
- Yamagami T, Tsuchisaka A, Yamada K, Haddon WF, Harden LA, Theologis A. 2003. Biochemical diversity among the 1-amino-cyclopropane-1-carboxylate synthase isozymes encoded by the Arabidopsis gene family. *J Biol Chem* 278(49): 49102–49112. [PubMed: 12968022]
- Yoon GM, Kieber JJ. 2013. 1-Aminocyclopropane-1-carboxylic acid as a signalling molecule in plants. *AoB PLANTS* 5.
- Young ME, Carroad PA, Bell RL. 1980. Estimation of diffusion coefficients of proteins. *Biotechnology and Bioengineering* 22(5): 947–955.
- Zamora O, Schulze S, Azoulay-Shemer T, Parik H, Unt J, Brosche M, Schroeder JI, Yarmolinsky D, Kollist H. 2021. Jasmonic acid and salicylic acid play minor roles in stomatal regulation by CO₂, abscisic acid, darkness, vapor pressure deficit and ozone. *Plant J* 108(1): 134–150. [PubMed: 34289193]
- Zhang J, De-Oliveira-Ceciliato P, Takahashi Y, Schulze S, Dubeaux G, Hauser F, Azoulay-Shemer T, Toldsepp K, Kollist H, Rappel WJ, et al. 2018. Insights into the Molecular Mechanisms of CO₂-Mediated Regulation of Stomatal Movements. *Current Biology* 28(23): R1356–R1363. [PubMed: 30513335]
- Zhang TY, Li ZQ, Zhao YD, Shen WJ, Chen MS, Gao HQ, Ge XM, Wang HQ, Li X, He JM. 2021. Ethylene-induced stomatal closure is mediated via MKK1/3-MPK3/6 cascade to EIN2 and EIN3. *J Integr Plant Biol* 63(7): 1324–1340. [PubMed: 33605510]
- Zhou J, Rocklin AM, Lipscomb JD, Que L Jr., Solomon EI. 2002. Spectroscopic studies of 1-aminocyclopropane-1-carboxylic acid oxidase: molecular mechanism and CO₂ activation in the biosynthesis of ethylene. *J Am Chem Soc* 124(17): 4602–4609. [PubMed: 11971707]

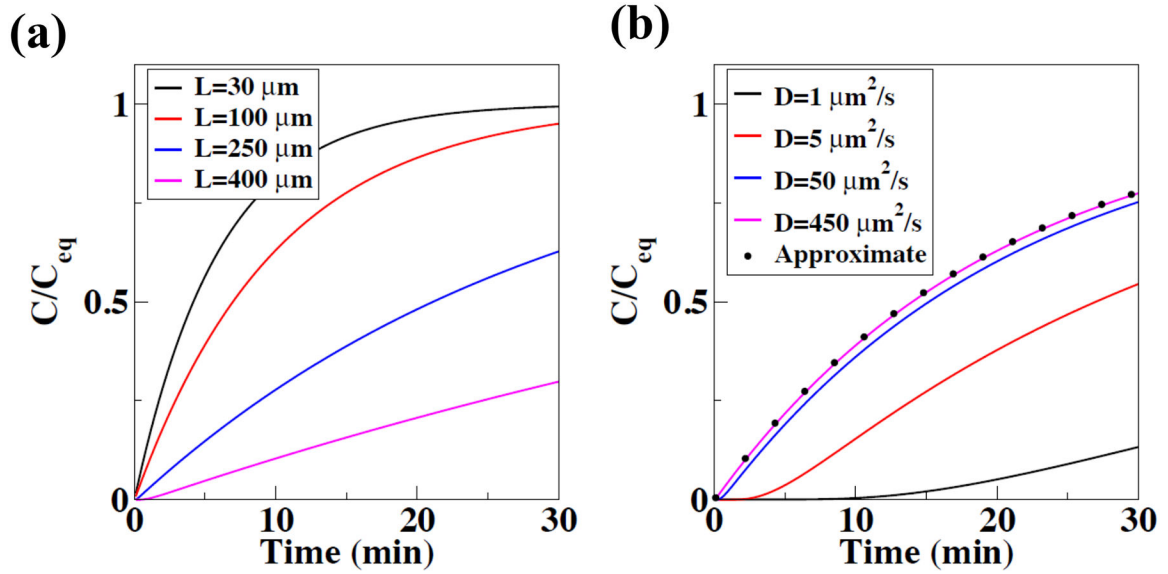


Fig. 1: Analytical model determines concentrations of signaling molecules at the guard cell surface.

(a) Analytical solution for the concentration, C , of a small molecule diffusing from a source (mesophyll) to the epidermis (guard cells) as a function of time following stimulation of the mesophyll and changing the model parameter representing the mesophyll-epidermis distance, L . The solution is rescaled by its steady state value, C_{eq} . Other model parameters are fixed ($D=450 \mu\text{m}^2/\text{s}$ and $\alpha=5 \mu\text{m}/\text{min}$) (see Results for details). (b) Analytical solution for the concentration C , rescaled by C_{eq} for a fixed length $L=100 \mu\text{m}$ and a range of values for the diffusion constant D , demonstrating that for large values of the diffusion coefficient D (here $D \geq 50 \mu\text{m}^2/\text{s}$) the dynamics of the concentration at the epidermal/guard cell surface C is not determined by the diffusion coefficient D (see Results for details). The remaining parameters are the same as in (a). However, for smaller diffusion coefficients, as have been measured in plant cell walls, the time of a small molecule to reach the epidermis/guard cells is considerably slowed (here $D \leq 50 \mu\text{m}^2/\text{s}$). The symbols (dots in panel b) correspond to the “approximate” analytical solution, valid for large diffusion constants, such as for gases in air and small soluble molecules in solution (see Methods and Results).

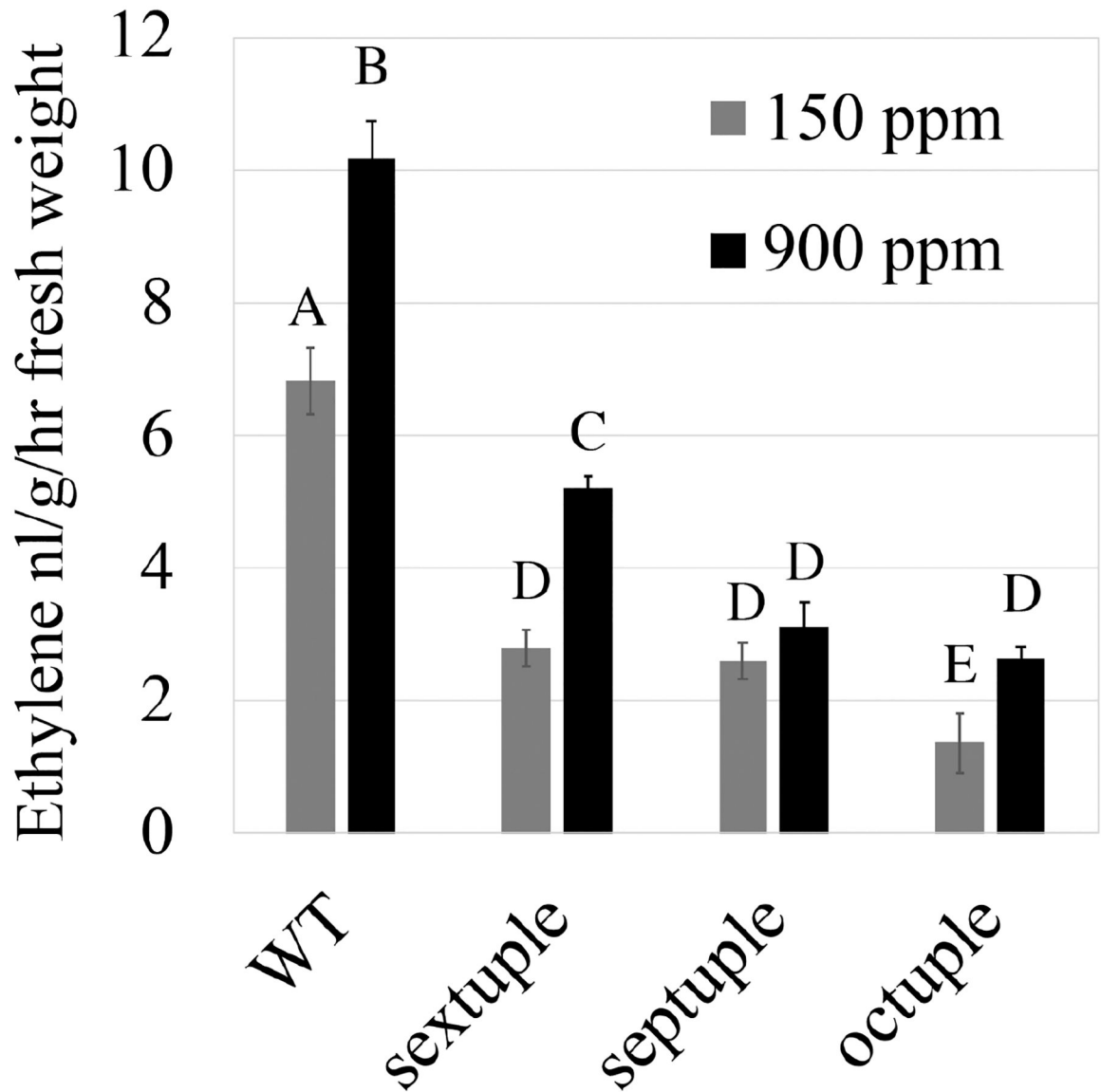


Fig. 2: CO₂-dependent ethylene production is impaired in higher-order *acs* mutant in response to elevated and low [CO₂].

Five-week-old *A. thaliana* wild-type (WT), ACC synthase (*acs*) sextuple, septuple and octuple mutant plants were incubated for 90 min under low (150 ppm) or high (900 ppm) [CO₂]. Ethylene production in *A. thaliana* rosettes was quantified using gas chromatography (n=6 replicates per each line and each treatment, where 2 whole *A. thaliana* rosettes were measured in each replicate). Different letters above bars indicate statistical differences between lines and treatments ($P < 0.05$, Two-way ANOVA). Similar results were found in 3 independent experiments. See Fig. S1 for additional independent experiments.

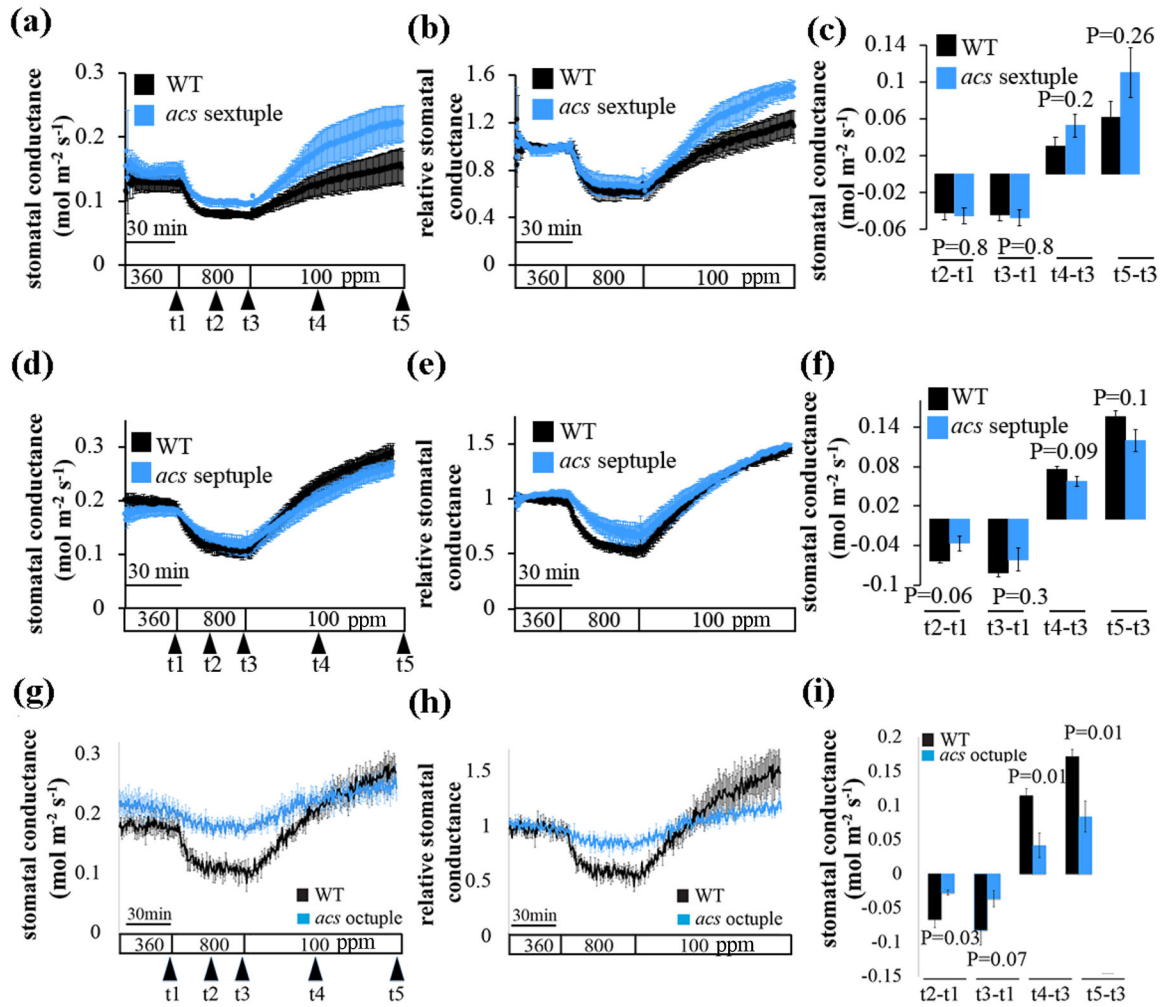


Fig. 3: CO₂-induced stomatal movements are severely affected in *acs* octuple mutant plant leaves but not in the *acs* sextuple and *acs* septuple mutants.

The graphs show average stomatal conductance of wild-type (WT, Col-0), (a-c) *acs* sextuple (n=3), (d-f) *acs* septuple (n=4), and (g-i) *acs* octuple (n=3) *A. thaliana* mutant leaves from intact plants in response to shifts in imposed [CO₂] as indicated at the bottom (ppm). (a, d and g) show stomatal conductance means (±SEM) of intact leaves from individual plants per genotype. (b, e, and h) Stomatal conductance (in panels a, d and g) were normalized to the stomatal conductance at 360 ppm [CO₂] before shifting to 800 ppm [CO₂]. (c, f and i) Changes in absolute stomatal conductance (mean ± SEM) were calculated at the indicated time points based on the data presented on panels a, d and g (t1=stomatal conductance at 360 ppm [CO₂], t2=15 min after shifting to 800 ppm [CO₂], t3=30 min after shifting to 800 ppm [CO₂], t4=40 min after shifting to 100 ppm [CO₂], t5=80 min after shifting to 100 ppm [CO₂]). Statistical analyses were done using unpaired Student's *t* tests between the wild-type and the mutant line, P-value is presented above/under columns. Note, wild-type control gas exchange data presented in panels g-i are the same as shown in Fig. S2 a-c and d-f, as these mutants were investigated within the same experimental set. Comparable results were found in 3 experiments. (See also Fig. S2).

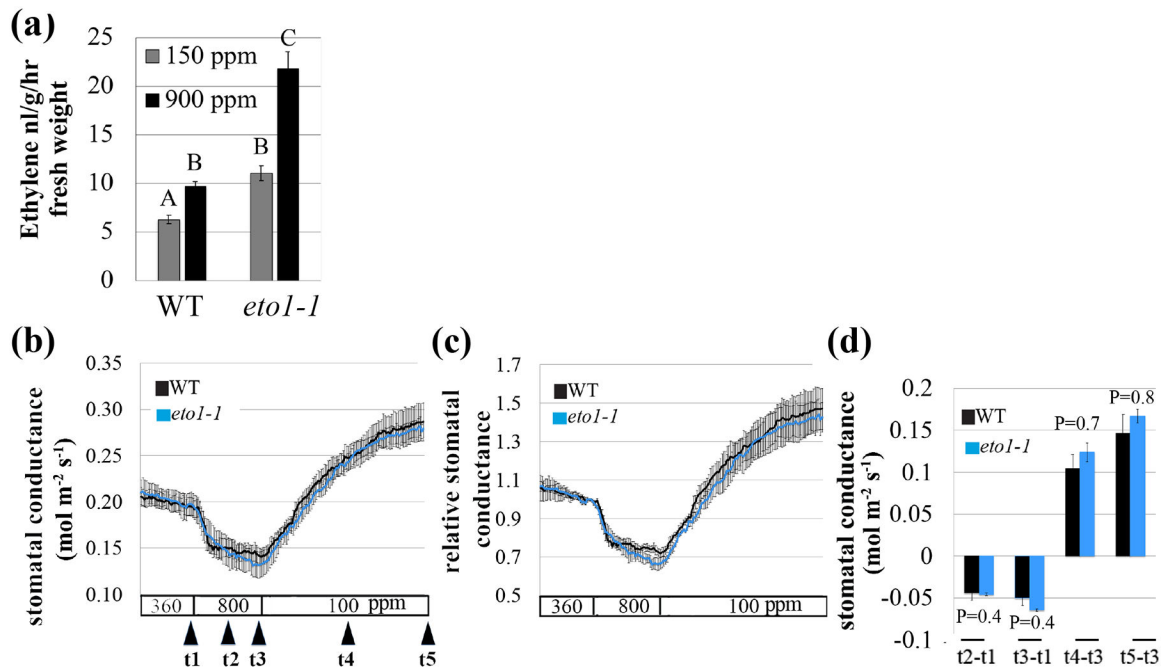


Fig. 4: Leaves of the ethylene overproducer, *eto1-1*, show intact CO₂-induced stomatal conductance responses.

A. thaliana wild-type (WT, Col-0) and the *eto1-1* mutant plants were grown under ambient CO₂ (400 ppm) for five-weeks and then measured for their (a) Ethylene levels using gas chromatography and (b) stomatal conductance responses to [CO₂]-shifts. (a) Potted plants were split into two groups and incubated at either low CO₂ (150 ppm) or high CO₂ (900 ppm) for 100 min. Ethylene production was then quantified using gas chromatography. Data present the mean of three independent experiments (n=8 plants in each experiment, for each line and condition). Letters indicate statistical differences between lines and treatment ($P < 0.05$, Two-way ANOVA). (b, c, d) Stomatal conductance of wild-type (WT, Col-0) and *eto1-1* *A. thaliana* mutant leaves from intact plants in response to shifts in imposed [CO₂] as indicated at the bottom (ppm). (b) Shown are mean (\pm SEM) of n=4 leaves from individual plants per genotype. (c) Stomatal conductance (in panel b) was normalized to the stomatal conductance at 360 ppm [CO₂] before shifting to 800 ppm [CO₂]. (d) Changes in absolute stomatal conductance (mean \pm SEM) were calculated at the indicated time points based on the data presented in panel b (t1=stomatal conductance at 360 ppm [CO₂], t2=10 min following exposure to 800 ppm [CO₂], t3=20 min following exposure to 800 ppm [CO₂], t4=25 min following exposure to 100 ppm [CO₂], t5=50 min following exposure to 100 ppm [CO₂]). Statistical analyses were done using unpaired Student's *t* tests between the wild-type and the mutant line, P-value is presented above/under columns. Comparable findings were made in additional independent experiments, using a different [CO₂]-shift protocol, where the gas exchanged leaf was exposed to ambient, low and then high CO₂ (Fig. S3).

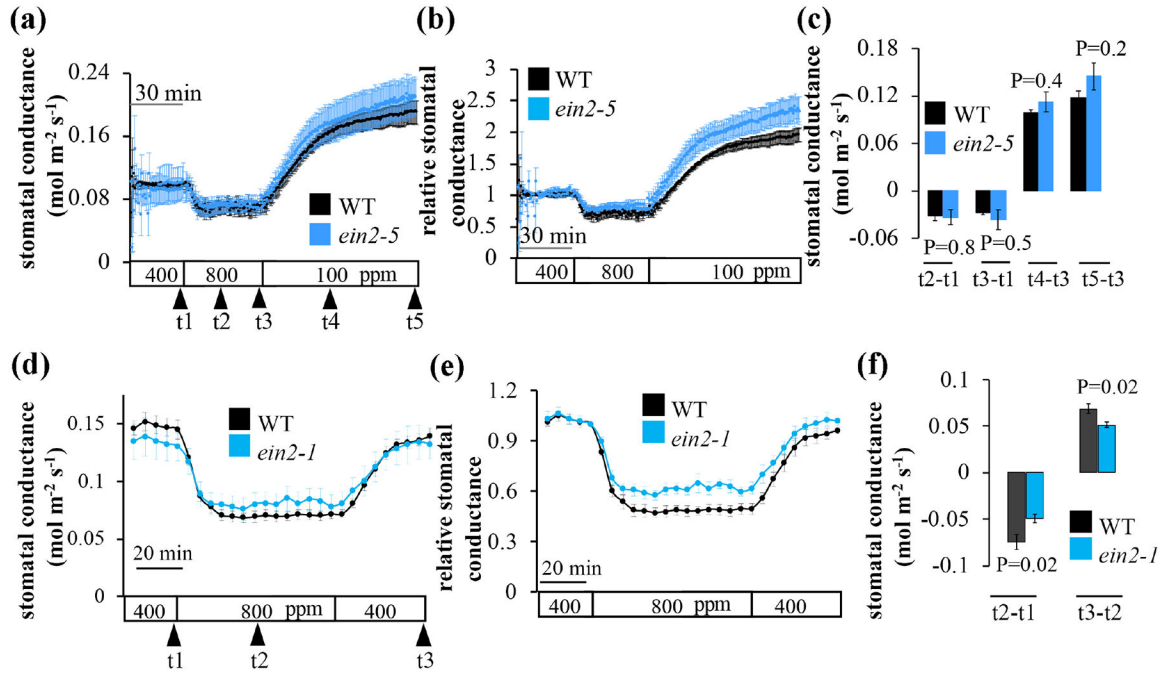


Fig. 5: Leaves of the ethylene insensitive signaling mutants, *ein2-5* and *ein2-1*, show CO₂-induced stomatal conductance responses.

The graphs show average leaf stomatal conductance from intact plants of wild-type (WT, Col-0), (a-c) *ein2-5* or (d-f) *ein2-1* *A. thaliana* mutant plants in response to [CO₂]-shifts, as indicated at the bottom (ppm). (a, d) Stomatal conductance means (±SEM) of (a) intact leaves (n=3) from individual plants or (d) whole intact plants (n=4) per genotype. (b, e) Stomatal conductance (in panels a and c) were normalized to the stomatal conductance at 400 ppm [CO₂] before shifting to 800 ppm [CO₂]. (c, f) Changes in absolute stomatal conductance (mean ± SEM). (c) Changes in absolute stomatal conductance (mean ± SEM) were calculated at the indicated time points based on the data presented in panel a (t1=stomatal conductance at 400 ppm [CO₂], t2=20 min following exposure to 800 ppm [CO₂], t3=40 min following exposure to 800 ppm [CO₂], t4=25 min following exposure to 100 ppm [CO₂], t5=50 min following exposure to 100 ppm [CO₂]) and d (t1 at 400 ppm [CO₂], t2=32 min following exposure to 800 ppm [CO₂], t3=last data point measured at 400 ppm [CO₂]). Statistical analyses were done using unpaired Student's *t* tests between the wild-type and the mutant line, P-value is presented above/under columns. Comparable results were found in additional independent experiments (e.g., Fig. S4).

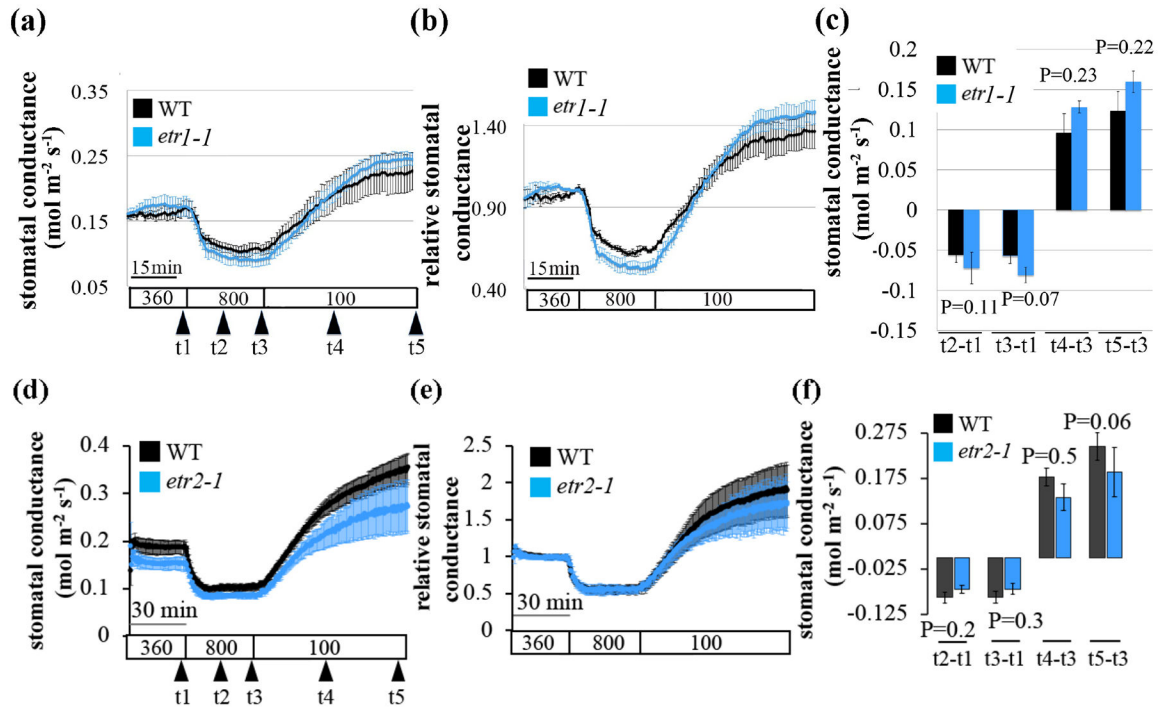


Fig. 6: Leaves of the ethylene insensitive receptor mutants, *etr1-1* and *etr2-1*, show intact CO₂-induced stomatal conductance responses.

The graphs show average leaf stomatal conductance from intact plants of wild-type (WT, Col-0), (a-c) *etr1-1* and (d-f) *etr2-1* *A. thaliana* mutant plants in response to [CO₂]-shifts, as indicated at the bottom (ppm). (a, d) Stomatal conductance means (\pm SEM) of n=4 leaves from individual plants per genotype. (b, e) Stomatal conductances (in panel a and d) was normalized to the stomatal conductance at 360 ppm [CO₂] before shifting to 800 ppm [CO₂]. (c, f) Changes in absolute stomatal conductance (mean \pm SEM) were calculated at the indicated time points based on the data presented in panel a (t1=stomatal conductance at 360 ppm [CO₂], t2=15 min following exposure to 800 ppm [CO₂], t3=30 min following exposure to 800 ppm [CO₂], t4=40 min in a / 30 min in b, following exposure to 100 ppm [CO₂], t5= last data point ~80 min following exposure to 100 ppm [CO₂]). Statistical analyses were done using unpaired Student's *t* tests between the wild-type and the mutant line, P-value is presented above/under columns. Similar findings were made in additional independent experiments (e.g., Fig. S5).

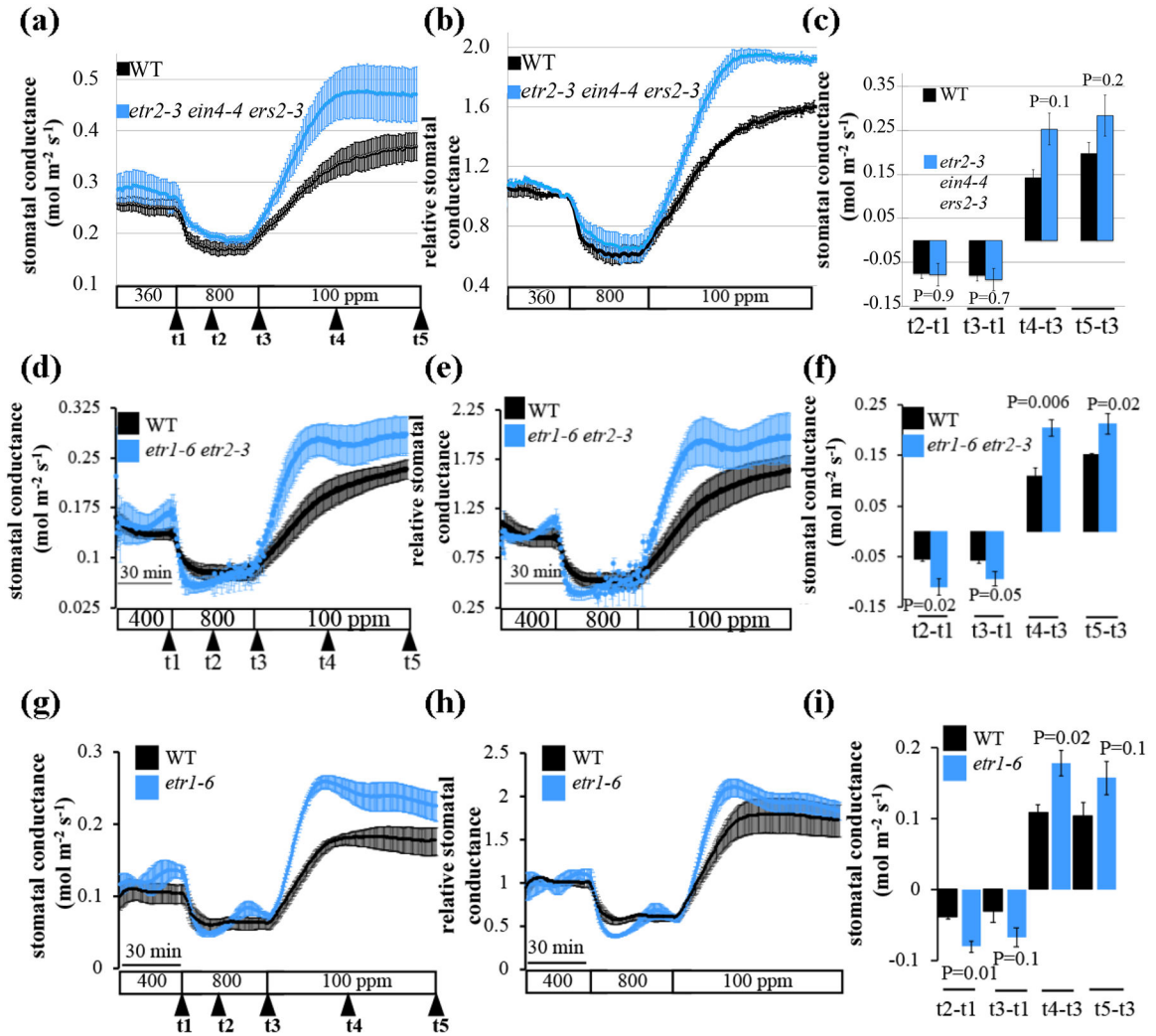


Fig. 7: Leaves of the ethylene receptor hypersensitive mutants, *etr2-3;ein4-4;ers2-3* triple mutant, *etr1-6;etr2-3* double mutant and the *etr1-6* single mutant plants, show accelerated CO₂-induced stomatal conductance responses.

The graphs show average leaf stomatal conductance from intact plants of wild-type (WT, Col-0), (a-c) *etr2-3;ein4-4;ers2-3* triple mutant, (d-f) *etr1-6;etr2-3* double mutant, (g-i) *etr1-6* single mutant of *A. thaliana* in response to [CO₂]-shifts as indicated at the bottom (ppm). (a, d and g) Stomatal conductance means (\pm SEM) of (a-c) n=4 (WT), and n=3 (*etr2-3;ein4-4;ers2-3*), (d-f) n=3, (g-i) n=3 leaves from individual plants per genotype. (b, e and h) Stomatal conductance (in panels a, d and g) were normalized to the stomatal conductance at 400 ppm [CO₂] before shifting to 800 ppm [CO₂]. (c, f, and i) Changes in absolute stomatal conductance (mean \pm SEM) were calculated at the indicated time points based on the data presented on panels a, d and g (t1 = stomatal conductance at 400 ppm [CO₂], t2=15 min following exposure to 800 ppm [CO₂], t3=30 min following exposure to 800 ppm [CO₂], t4=40 min following exposure to 100 ppm [CO₂], t5=80 min following exposure to 100 ppm [CO₂]). Statistical analyses were done using unpaired Student's *t* tests between the wild-type and the mutant line, P-value is presented above/under columns.

Similar findings for the *etr1-6;etr2-3* double mutant were found in additional independent experiments (see Fig. S6).

Author Manuscript

Author Manuscript

Author Manuscript

Author Manuscript

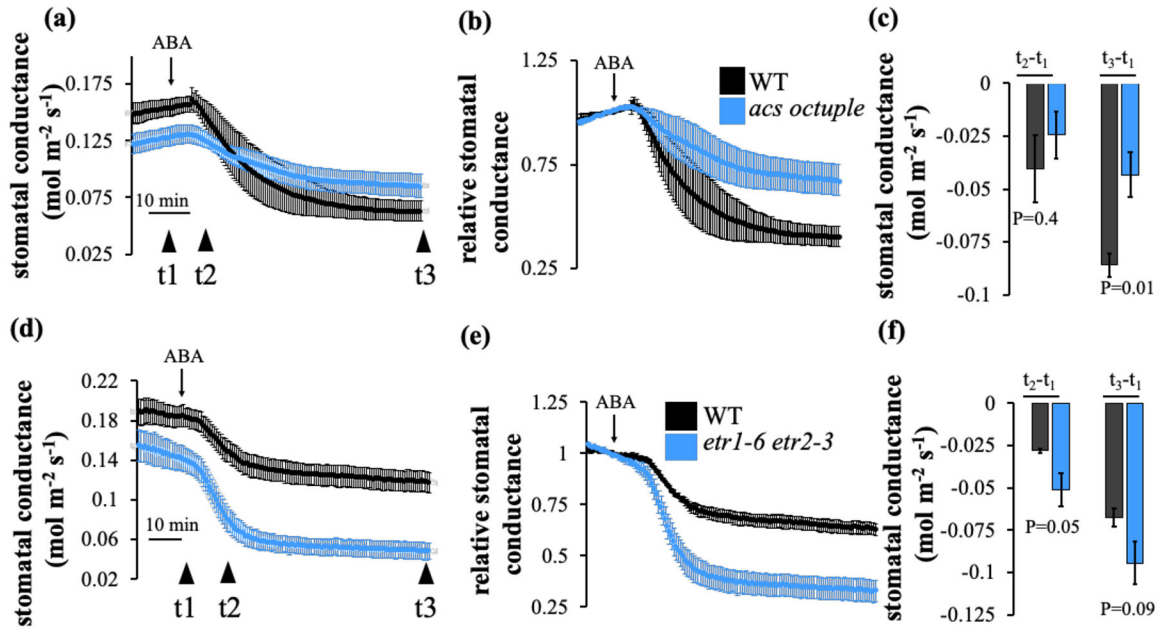


Fig. 8: ABA-induced stomatal closure is impaired in *acs octuple* mutant plant leaves, whereas ethylene receptor hypersensitive double mutant, *etr1-6;etr2-3* plants, show enhanced and accelerated ABA-induced stomatal closure.

Time-resolved stomatal conductance in response to 2 μ M ABA petiole-fed leaves in wild-type (WT, Col-0), (a-c) *acs octuple* and (d-f) *etr1-6;etr2-3* double mutant leaves. Stomatal conductance means (\pm SEM) of (a-c) $n=5$ (d-f) $n=4$ leaves from individual plants per genotype. (b, e) Stomatal conductance (in panels a and d) were normalized to the steady-state stomatal conductance before ABA was applied. (c and f) Changes in absolute stomatal conductance (mean \pm SEM) were calculated at the indicated time points based on the data in panels a and d (t_1 = steady-state stomatal conductance, $t_2=20$ min and $t_3=50$ min following application of ABA). Statistical analyses were done using unpaired Student's *t* tests between the wild-type and the mutant line, P-value is presented under columns. Experimental sets were repeated three times showing similar results.

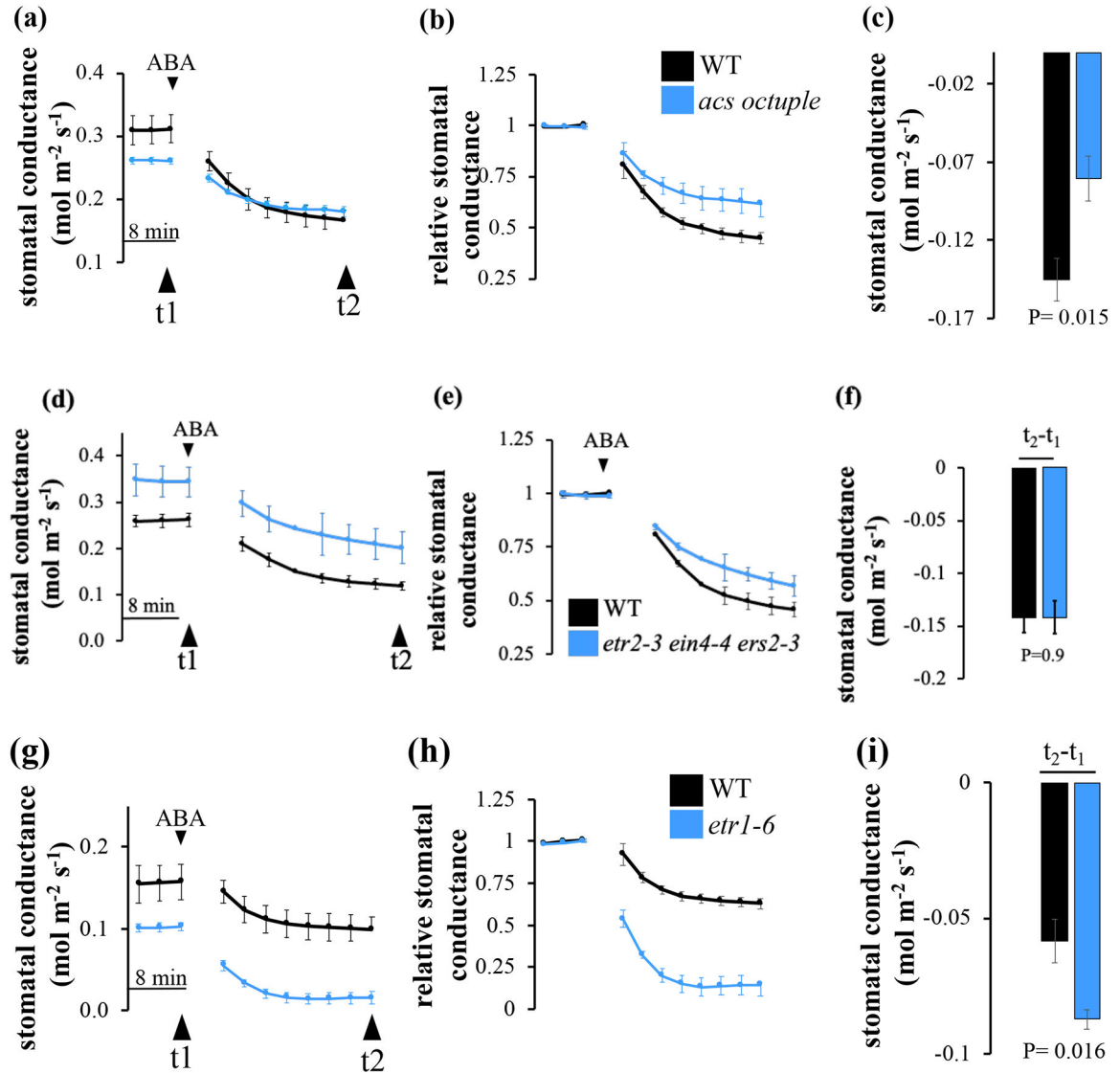


Fig. 9: ABA-induced stomatal closure is intact in the ethylene receptor hypersensitive triple mutant, *etr2-3; ein4-4; ers2-3*, while *etr1-6* mutant plants show enhanced ABA-induced stomatal closure.

Time-resolved stomatal-conductance in response to 5 μM ABA sprayed leaves in wild-type (WT, Col-0), (a-c) *acs octuple* (d-f) *etr2-3; ein4-4; ers2-3* triple mutant and (g-i) *etr1-6*. (a, d and g) Stomatal conductance means (\pm SEM) of $n=4$ leaves from individual plants per genotype. (b, e and h). Stomatal conductances (in panels a, d and g) were normalized to the steady-state stomatal conductance before ABA was applied). (c, f and i) Changes in absolute stomatal conductance (mean \pm SEM) were calculated at the indicated time points based on the data presented in panels a, d and g (t_1 = steady-state stomatal conductance, $t_2=20$ min following ABA spray). Statistical analyses were done using unpaired Student's t tests between the wild-type and the mutant line, P-value is presented above columns. Experimental sets were repeated three times showing similar results.